https://doi.org/10.5194/egusphere-2026-2415
Preprint. Discussion started: 6 May 2026
© Author(s) 2026. CC BY 4.0 License.

Extending planktic foraminiferal Mg/Ca palaeothermometry into polar temperature ranges: crust- and lamellae specific calibrations and non-thermal controls

Adele Westgård[1*], Mohamed M. Ezat[1], Freya E. Sykes[1], Julie Meilland[2,3], Thomas B. Chalk[1,3], J. Andy Milton[4], Melissa Chierici[5], Gavin L. Foster[4]

*Correspondence to: adele.westgard@uit.no

[1] iC3: Centre for ice, Cryosphere, Carbon and Climate, Department of Geosciences, UiT The Arctic University of Norway, 9037 Tromsø, Norway

[2] MARUM – Center for marine environmental sciences, University of Bremen, Leoberner str. 8 Bremen 28359, Germany

[3] Aix Marseille Université, CNRS, IRD, INRAE, CEREGE, Technopole Environnement Arbois-Méditerranée BP 80 13545 Aix-en-Provence, Cedex 04, France

[4] School of Ocean and Earth Science, National Oceanography Centre Southampton, University of Southampton, Southampton SO 3ZH, England

[5] Institute of Marine Research, Oceanography and Climate Research Group, Fram Centre, Hjalmar Johansens gate 14, 9007, Tromsø, Norway

https://doi.org/10.5194/egusphere-2026-2415
Preprint. Discussion started: 6 May 2026
© Author(s) 2026. CC BY 4.0 License.

Abstract

The rapidity of climate change in the polar regions underscores the need for improved understanding of its impacts on ocean circulation at both regional and global scales. Reconstructions of past polar ocean-cryosphere interactions can provide this context, but large uncertainties in existing proxies limit the utility of such studies. For instance, there are currently no low-temperature (<9°C) culture-based Mg/Ca-calibrations for planktic foraminifera, a key tool for reconstructing past changes in ocean temperatures. There is also limited understanding of non-thermal influences on Mg/Ca in *Neogloboquadrina pachyderma,* the only modern polar planktic foraminifera. Moreover, this species exhibits considerable levels of heterogeneity in composition precipitating a thick lower-Mg/Ca outer crust over higher Mg/Ca inner lamellae calcite; specimens with predominantly, albeit variable crust–lamellae proportions, are thus thought to introduce substantial uncertainty into high-latitude palaeotemperature reconstructions. Here, we used *N. pachyderma* cultured across a range of temperatures, salinities, and carbonate chemistry conditions including experiments in which pH and [CO_3^{2-}] either covaried or were decoupled. By using a laser ablation approach to analyse crust and lamellae separately, we present new Mg/Ca-temperature calibrations for each component that extend culture-based calibrations in *N. pachyderma* down to the lower temperature-range (2–9°C). The crust-specific calibration is of particular importance in high-latitude downcore records where *N. pachyderma* are commonly observed to preserve predominantly or only crust. Our results show significant carbonate chemistry influence on Mg/Ca with opposite influences from pH and carbonate ion concentration, when these variables changed in isolation. Additionally, we show that environmental conditions regulate crust-lamellar proportions, where increased salinity and temperature, and lower pH lead to less crust formation with implications for future ocean acidification and Arctic Atlantification, and for downcore reconstructions.

https://doi.org/10.5194/egusphere-2026-2415
Preprint. Discussion started: 6 May 2026
© Author(s) 2026. CC BY 4.0 License.

1 Introduction

Understanding of polar surface ocean hydrography, and ocean-cryosphere interactions are crucial to assessing the implications of ongoing high-latitude warming. Studying past climate change in the polar regions provides invaluable insights into these processes (e.g., Ezat et al., 2024; Stein, 2019; Hou et al., 2025). However, there are several challenges to studying polar palaeoceanography, including limited access due to the remoteness and prolonged sea ice cover, low sedimentation rates of deep ocean sediments, and preservation biases of common proxy carriers such as the dissolution of calcareous fossils (e.g., Stein, 2019). This is particularly true for the magnesium to calcium ratio (Mg/Ca) of foraminifera shells, a key proxy used to reconstruct paleotemperature (e.g., Elderfield and Ganssen, 2000), that results in a range of unrealistic values in the polar regions when applying existing calibrations (e.g., Prabhakar et al., 2024).

The polar planktic foraminifera *Neogloboquadrina pachyderma* is the most abundant species of planktic foraminifera in the high latitude oceans and often the only planktic species available in polar sedimentary records (e.g., Chaabane et al., 2024; Kucera, 2007). It is therefore a key species for reconstructing past surface hydrography in the high latitudes (Eynaud et al., 2009; Kohfeld et al., 1996; Rodríguez-Sanz et al., 2012). Its habitat extends from equatorial upwelling zones to polar waters, and dominates the planktic foraminifera assemblage at temperatures <5°C (Greco et al., 2019; Kucera et al., 2005; Anglada-Ortiz et al., 2023). Studies have also suggested that *N. pachyderma* adjusts its depth habitat in response to food-availability and productivity, sea-ice, and sea surface temperature (SST) hence reducing its representation of actual SSTs (Greco et al., 2019; Anglada-Ortiz et al., 2023). *N. pachyderma* is a resilient and opportunistic species which has been found to: live in sea ice, in marine snow/aggregate microhabitats, and utilise behaviours such as dormancy, ectoplasmic structures, and asexual reproduction to survive unfavourable conditions and/or quickly recover its population (e.g., Greco et al., 2023; Meilland et al., 2022; Westgård et al., 2023; Davis et al., 2020; Spindler and Dieckmann, 1986). These strategies may impact the environmental signals recorded by its shell geochemistry through, for example, extended life cycle due to dormancy and extreme habitat conditions

https://doi.org/10.5194/egusphere-2026-2415
Preprint. Discussion started: 6 May 2026
© Author(s) 2026. CC BY 4.0 License.

(e.g., high salinity, high pH) in the sea ice (Spindler and Dieckmann, 1986; Bertlich et al., 2021; Westgård et al., 2023).

The combination of biological processes and life cycle behaviours of foraminifera cause a range of non-environmental variability in shell geochemical composition often referred to as the collective term "vital effects" (e.g., Kozdon et al., 2009b; Branson et al., 2025). In *N. pachyderma* this arises from, for example, the thick crust it forms towards the end of its life cycle covering the outer portions of its shell with a markedly different geochemical composition from the initial lamellar calcite (Hupp and Fehrenbacher, 2023, 2024; Jonkers et al., 2016; Kozdon et al., 2009a; Kozdon et al., 2009b; Westgård et al., 2026). For instance, it is commonly observed that the Mg/Ca ratio of the crust is substantially lower than the lamellar calcite (Hupp and Fehrenbacher, 2023, 2024; Jonkers et al., 2016; Kozdon et al., 2009a; Livsey et al., 2020; Davis et al., 2017; Westgård et al., 2026).

Westgård et al. (2026) showed that when the crust and lamellar calcite grew in the same environmental conditions, the observed geochemical difference persisted, implying the observed compositional variations resulted from contrasting biomineralisation processes rather than environmental influences from, for example, vertical migration in the water column. For any given Mg/Ca calibration, the lower Mg/Ca crust yields lower temperatures than the higher Mg/Ca lamellar calcite from the same specimen and population, even when grown at equivalent conditions. The laboratory-based study also found that the difference between the two components decreases with increasing temperature and is insignificant at the higher temperatures inhabited by the species (Westgård et al., 2026). As Mg/Ca increases exponentially with temperature, Mg/Ca-temperature calibrations are less sensitive at the lower temperature-range. The larger difference between crust and lamellar calcite Mg/Ca at lower temperatures therefore lead to additional uncertainties in temperature estimates based on both components.

The geochemistry of the test is often dominated by the crust, that accounts for ~40–80% of the total shell mass (e.g., Kozdon et al., 2009a; Hupp and Fehrenbacher, 2023) and can vary within and between samples downcore (Westgård et al., 2026). The varying ratio between the two components makes it challenging to account for the geochemical difference between the crust and lamellar calcite, for

https://doi.org/10.5194/egusphere-2026-2415
Preprint. Discussion started: 6 May 2026
© Author(s) 2026. CC BY 4.0 License.

example by assuming a constant volume fraction. The difference in geochemical composition between the two components, and the proportion of crust are therefore underappreciated sources of inaccuracy and uncertainty in *N. pachyderma* and must be considered in application and development of geochemical proxy calibrations.

Westgård et al. (2026) proposed a method to separate the two components in element/Ca profiles obtained from Laser Ablation Inductively Coupled Plasma Mass Spectrometry (LA ICP-MS) which opened the possibility of developing and applying proxy-calibrations for the two components independently. This is in line with previous studies, which suggests that using the components separately can reduce uncertainty and inaccuracy in temperature estimates (e.g., Livsey et al., 2020; Jonkers et al., 2016).

Most existing calibrations of the Mg/Ca temperature relationship (Table 1) are based on whole-shell measurements of *N. pachyderma* (and other species) from core top or sediment trap samples (e.g., Anand et al., 2003; Elderfield and Ganssen, 2000; Kozdon et al., 2009a; Vázquez Riveiros et al., 2016; Lea et al., 1999; Jonkers et al., 2013) or a combination of tow, sediment trap, core top, and/or culture samples (Morley et al., 2024; Tierney et al., 2019). Although, there are two Mg/Ca calibrations based on the lamellar calcite only from plankton tow and laboratory-grown specimens (c.f., Livsey et al., 2020; Davis et al., 2017). There are however currently no culture-based Mg/Ca calibrations below 9°C (see Table 1) for *N. pachyderma* and no calibrations that consider the crust only, or both components calcite independently. This is desirable because the crust component is the largest, by mass, and the lamella component is preferentially lost during sample cleaning and early diagenesis (c.f., Fritz-Endres and Fehrenbacher, 2021).

Other environmental factors have also been shown to influence the Mg/Ca ratio in foraminifera, e.g., salinity (Hönisch et al., 2013; Peral et al., 2022; Allen et al., 2016) and seawater carbonate chemistry (e.g., Allen et al., 2016; Holland et al., 2020; Morley et al., 2024; Russell et al., 2004; Evans et al., 2016; Haynes et al., 2023). Some authors have developed calibrations which consider corrections for such non-thermal influences on Mg/Ca in *N. pachyderma* and other species (e.g., Morley et al., 2024; Tierney et al., 2019; Davis et al., 2017).

https://doi.org/10.5194/egusphere-2026-2415
Preprint. Discussion started: 6 May 2026
© Author(s) 2026. CC BY 4.0 License.

Because only a few culture studies exist for *N. pachyderma,* and to our knowledge only one study, Westgård et al. (2026), document geochemical signals in laboratory-grown crust, the influence of the aforementioned thermal and non-thermal influences on Mg/Ca in both the crust and lamellar calcite remain poorly constrained.

Here we present Mg/Ca-environmental relationships from extensive culture experiments (Table S1 and 2) conducted in 2021 and 2022 across a range of temperatures (2–9°C), carbonate chemistry ($[CO_3^{2-}]$ 64–243 µmol/kg; pH 7.65–8.4), and salinities (29.8–36.7) encompassing realistic past and future conditions of the polar environments (e.g., Amap, 2018; Stein, 2019). The results presented in this study are produced using the data processing method presented in Westgård et al. (2026, Table S1). Mg/Ca data from all salinities, carbonate chemistries, and temperatures 2 and 7°C, and all Mg/Ca-environmental parameter relationships are presented for the first time in this study (Table S1). Mean Mg/Ca from temperature treatments 4.5, 6, and 9°C were first presented in Westgård et al. (2026) in relation to method development and studying the differences between crust and lamellae calcification (Table S1) and are available through the open data repository DataverseNO at: https://doi.org/10.18710/IYDI4O. Biological observations from 2021 experiments are presented in Westgård et al. (2023, Table S1).

By using a laser ablation approach, we provide new *N. pachyderma* Mg/Ca-temperature calibrations for polar conditions with separate calibrations for the crust and lamellar calcite (Table S1). In addition to thermal influences, we quantify the effects of salinity and carbonate chemistry on Mg/Ca.

https://doi.org/10.5194/egusphere-2026-2415
Preprint. Discussion started: 6 May 2026
© Author(s) 2026. CC BY 4.0 License.

Table 1. A selection of existing Mg/Ca-based temperature calibrations. T = temperature, S = salinity, N = sample size, ΩCa = calcite saturation state, $[CO_3^{2-}]$ = carbonate ion concentration, *N. p.* = *Neogloboquadrina pachyderma*, *N. i.* = *Neogloboquadrina incompta*. See also Fig. 4.

Study	Equation Mg/Ca (mmol/mol) =	T range (°C)	Culture/ tow/ coretop/ sediment trap	Other environmental factors (S, pH, $[CO_3^{2-}]$)	Species	N	Solution/ laser	Crust/ lamellar/ both	Notes
(Livsey et al., 2020)	$1.93*\exp^{(0.082T)}$	-1.81 to 3.80	tow		*N. p.*	41	laser	lamellar	
(Kozdon et al., 2009a)	0.13T + 0.35	>3, 3-6	Core top	$\delta^{44/40}Ca$ for depth	*N. p.*	20 with 60–80 specimens	solution	both	
(Jonkers et al., 2013)	$0.60*\exp^{(0.09T)}$	5-10	Sediment trap		*N. p.*	20 samples of 20–40 specimens	solution	both	
(Tierney et al., 2019)	BAYMAG code on github	-0.9 to 15.3	Culture + coretop	S, pH, bottom water ΩCa	Multi and N. p. + N. i.	119 + 12	both	both	Baysian model
(Morley et al., 2024)	$Mg/Ca_{[CO32-]} = 3227.95*[CO_3^{2-}]^{-1.53}$ $Mg/Ca[corr] = 0.327\exp^{(0.0936T)}$	-2 to 16	Tow + core top	$[CO_3^{2-}]$	*N. p.* + *N. i*	235	solution	Both, correction -15%	Requires $[CO_3^{2-}]$ proxy ($\delta^{18}O$)
(Davis et al., 2017)	0.71*T – 2.49	(6) 9 - 12	culture		*N. p.*	10	laser	lamellar	No chamber addition was reported at 6°C, thus there is large uncertainty in the calibration below 9°C.

https://doi.org/10.5194/egusphere-2026-2415
Preprint. Discussion started: 6 May 2026
© Author(s) 2026. CC BY 4.0 License.

2 Methods

Sample collection and experiments were conducted during summers 2021 and 2022 and specimens were sampled from 74.5°N, 01.6°E (Ezat et al., 2021) and 72.5°N, 00.0°E (Ezat et al., 2022) aboard the RV Helmer Hanssen. The protocol of sample collection and culture methods for 2021 experiments are presented in Westgård et al. (2023) and culture protocol for temperatures 6 and 9°C (2022) experiments and trace element analysis are presented in Westgård et al. (2026). See overview in Table S1. All experimental procedures were similar and are described herein for completeness.

2.1 Foraminifera sampling and culturing

Small (<120 µm), healthy specimens (i.e., with bright orange cytoplasm and extensive rhizopodial network) of *Neogloboquadrina pachyderma* were collected using a WP2 plankton net (64µm mesh) and placed into individual 70 mL culture bottles pre-filled with culture media (chemistry controlled filtered sea water). Upon return to the laboratory at UiT The Arctic University of Norway, specimens were placed into light and temperature-controlled Friocell EVO incubators set at 2–9°C (see detailed culture conditions in Table 2). Water treatments were prepared with independently variable parameters intended to reflect realistic past and future conditions with salinities of 29.8–36.7, pH of 7.65–8.4 (total scale), $[CO_3^{2-}]$ of 64–243 µmol/kg, where we also altered pH and $[CO_3^{2-}]$ independently of each other.

To ensure calcification only occurred in intended conditions, water was replaced every 2–6 days and. experiments were terminated in case of any pH drift >0.05 from the intended value. Dead specimens (i.e. shells appearing empty) were rinsed in distilled water and placed individually in micropalaeontological slides.

2.2 Preparation and monitoring of culture media:

Seawater for culture media was immediately filtered (2 µm cellulose filters) and stored in opaque 20L cans at 4°C. Water samples were collected for elemental composition (Table 3) and carbonate chemistry

https://doi.org/10.5194/egusphere-2026-2415
Preprint. Discussion started: 6 May 2026
© Author(s) 2026. CC BY 4.0 License.

(Table 2, Fig. S1) prior to, during, and at the end of the experiments. Each set of experiments had a dedicated "ambient" treatment (pH ~8.1, salinity ~35 and temperature 4.5ºC in 2021 and 6ºC in 2022), with conditions closely matching those at the foraminiferal collection site. Salinity and carbonate chemistry experiments were performed at two different temperatures, i.e., 4.5°C (2021) and 6°C (2022).

Incubator temperatures were set to 2, 4.5, 6, 7, and 9°C (Table 2) and remained stable throughout the experiments. Instrumentation error is <0.5°C spatially and <0.2°C temporally. The LED light programme was set to mimic the high-latitude summer conditions.

Salinity of the culture media (Table 2) was increased by adding brine from partial freezing of filtered seawater and lowered by the additional of the melt of the ice fraction with the aim to replicate conditions produced during sea ice formation as closely as possible. For the salinity experiments performed in 2021, salinity was also decreased by addition of distilled water and increased by addition of brine produced from evaporation of seawater on a hotplate (c.f., Westgård et al., 2023). This resulted in seven treatments with variable salinity: 29.8, 32.5, 33.6, 36.7 (from the partial freezing of seawater approach), 30.4 and 32.1 (addition of distilled water), 36.7 (brine from evaporated seawater), plus the two ambient treatments at 35.0 (4°C), and 35.4 (6°C).

Carbonate chemistry of the culture media (Table 2) was modified in three ways with the intended outcomes of: 1) altering pH and other carbonate parameters by addition of HCl to decrease pH or NaOH to increase pH, resulting in concurrent changes in pH and carbonate ion concentration ($[CO_3^{2-}]$); 2) altering pH while forcing $[CO_3^{2-}]$ to remain constant by addition of HCl or NaOH and adjusting $[CO_3^{2-}]$ by addition of artificial seawater (a mixture of distilled water and salt) or $NaHCO_3$; or 3) altering $[CO_3^{2-}]$ while keeping pH stable, by addition of $NaHCO_3$ or artificial seawater.

This resulted in five treatments where pH and $[CO_3^{2-}]$ co-varied (pH 7.78, 7.83, 7.84, 8.04, 8.10, 8.26, and 8.40), three treatments of variable $[CO_3^{2-}]$ at stable pH (64, 195, 206 µmol/kg at pH 8.07±0.13) and three treatments with variable pH at relatively stable $[CO_3^{2-}]$ (pH 7.65, 7.88, 8.15 at $[CO_3^{2-}]$ = 129±22 µmol/kg).

Isotope labelling

https://doi.org/10.5194/egusphere-2026-2415
Preprint. Discussion started: 6 May 2026
© Author(s) 2026. CC BY 4.0 License.

All experimental water were labelled with ^{135}Ba-isotope spike where $^{135}Ba_{sw}$ 95 = % of total Ba, in order to distinguish laboratory-grown calcite from ocean-grown calcite, resulting in $^{135}Ba_{sw}$ of 1.16 µmol and 1.97 µmol in 2021 and 2022 respectively (c.f., Westgård et al., 2026).

2.3 Analysis of water samples:

Water samples taken for carbonate chemistry (Table 2, Fig. S1) and elemental composition (Table 3) were analysed at the Institute of Marine Research (IMR) in Tromsø, Norway and the Centre for Earth Research and Analysis (CERAS) at the University of Southampton, UK, respectively, for detailed procedures refer to Westgård et al. (2026).

Samples for determining carbonate chemistry were analysed for total alkalinity (TA) and dissolved inorganic carbon (DIC) following protocols described in Dickson et al. (2007). All other carbonate system parameters were calculated in CO2SYS software (CO2SYS program, Pierrot et al., 2006) with paired TA and DIC, salinity, and experimental temperature. Due to extreme high DIC in the pH 7.6 treatment with decoupled [CO_3^{2-}], total alkalinity (TA) was not measured. This variable and the remaining carbonate system parameters calculated from DIC measured at IMR were combined with pH on total scale measured during experiments using a handheld Metrohm 914 pH-meter at experimental temperature (6°C).

Water samples for element analysis were analysed using an Agilent 8900 Triple Quadrupole (QQQ) ICP-MS in He-gas mode to achieve acceptable sensitivity for Mg/Ca (Table S2). Based on analysis of the SOTON-SW internal sea water standard, the long-term accuracy for Mg, Ca, and Ba is <7%. Reproducibility is <10% (2SD) for Mg and Ca (at ≥0.2 ppm).

*Table 2. Water conditions including temperature, salinity, and carbonate chemistry, for all water treatments. The method used to modify salinity treatments is indicated in the "comments" column. *Ambient treatments for years 2021 and 2022,* with conditions closely matching those at the foraminiferal collection site. ***TA, HCO_3^-, and $\Omega_{calcite}$ are estimated values based on measured DIC, pH measured during experiments, and experimental temperature (see section 2.3); DIC, TA and pH were measured for all other treatments. See treatment correlations and scatter matrix of water treatments in Fig. S1. pH_T = pH on total scale, TA = total alkalinity, DIC = dissolved inorganic carbon, $[CO_3^{2-}]$ = carbonate ion concentration, $[HCO_3^-]$ = bicarbonate ion concentration, $\Omega_{calcite}$ = calcite saturation state, T = temperature.*

Variable	*Year*	*Salinity*	*DIC (µmol/kg)*	*TA (µmol/kg)*	*pH_T*	*$[CO_3^{2-}]$ (µmol/kg)*	*$[HCO_3^-]$ (µmol/kg)*	*$\Omega_{calcite}$*	*T (°C) ± <0.5*	*Comments*
Temperature	2021	35.0 ±0.7	2213 ±40	2391 ±20	8.16 ±0.05	130 ±12	2065 ±52	3.1 ±0.3	2	
	*2021	35.0 ±0.7	2213 ±40	2391 ±20	8.10 ±0.05	130 ±12	2065 ±52	3.1 ±0.3	4.5	
	*2022	35.4 ±0.1	2158 ±12	2338 ±22	8.04 ± 0.07	138 ±17	1997 ±35	3.3 ±0.4	6	
	2021	35.0 ±0.7	2213 ±40	2391 ±20	8.08 ±0.05	130 ±12	2065 ±52	3.1 ±0.3	7	
	2022	35.4 ±0.1	2158 ±12	2338 ±22	8.09 ± 0.07	138 ±17	1997 ±35	3.3 ±0.4	9	
salinity	2021	29.8 ±0.1	1902 ±28	2043 ±5	8.12 ±0.07	102 ±13	1784 ±39	2.5 ±0.3	4.5	Distilled water
	2022	30.4 ±0.1	1952 ±17	2051 ±1	7.96 ±0.05	86 ±9	1837 ±22	2.2 ±0.2	6	Melted «sea-ice»
	2021	32.1 ±0.1	2038 ±27	2197 ±8	8.12 ±0.05	115 ±11	1906 ±35	2.8 ±0.3	4.5	Distilled water
	2022	32.5 ±0.0	2127 ±21	2273 ±6	8.03 ±0.07	117 ±16	1985 ±34	2.8 ±0.3	6	Melted «sea-ice»
	2021	33.6 ±0.0	2136 ±20	2332 ±4	8.17 ±0.04	140 ±10	1980 ±28	3.4 ±0.2	4.5	Melted «sea-ice»
	2021	36.7 ±0.1	2330 ±16	2494 ±0	8.04 ±0.04	124 ±9	2184 ±23	2.9 ±0.2	4.5	Rejected brine
	2021	36.7 ±0.5	2267 ±21	2439 ±25	8.07 ±0.01	127 ±3	2120 ±18	3.0 ±0.1	4.5	Evaporated brine
pH and carbonate ion concentration	2022	35.4 ±0.1	2177 ±35	2241 ±24	7.78 ±0.04	73 ±6	2059 ±35	1.8 ±0.1	6	
	2022	35.3 ±0.1	2183 ±8	2264 ±2	7.83 ±0.03	82 ±5	2061 ±10	2.0 ±0.1	6	
	2021	35.0 ±0.1	2193 ±35	2270 ±21	7.84 ±0.04	72 ±17	2087 ±48	1.7 ±0.4	4.5	
	2022	35.4 ±0.1	2300 ±40	2583 ±3	8.26 ±0.07	211 ±24	2073 ±62	5.1 ±0.6	6	
	2021	35.0 ±0.1	2218 ±8	2567 ±5	8.40 ±0.01	243 ±2	1966 ±9	5.8 ±0.0	4.5	
Carbonate ion concentration	2022	36.7 ±0.1	1641 ±22	1716 ±3	7.83 ±0.08	64 ±11	1547 ±27	1.5 ±0.3	6	
	2022	35.4 ±0.2	2890 ±11	3124 ±5	8.12 ±0.02	195 ±8	2668 ±17	4.7 ±0.2	6	
	2022	35.2 ±0.2	3406 ±14	3635 ±1	8.07 ±0.02	206 ±9	3163 ±21	4.9 ±0.2	6	
pH (decoupled carbonate ion concentration)	**2022	35.4 ±0.1	4772 ±10	4800	7.65	129	4514	3.1	6	
	2022	35.2 ±0.2	3558 ±10	3688 ±1	7.88 ±0.02	147 ±6	3352 ±13	3.5 ±0.1	6	
	2022	36.8 ±0.4	1229 ±19	1388 ±2	8.15 ±0.05	93 ±8	1126 ±26	2.2 ±0.2	6	

https://doi.org/10.5194/egusphere-2026-2415
Preprint. Discussion started: 6 May 2026
© Author(s) 2026. CC BY 4.0 License.

https://doi.org/10.5194/egusphere-2026-2415
Preprint. Discussion started: 6 May 2026
© Author(s) 2026. CC BY 4.0 License.

2.4 Foraminiferal sample preparation and Laser Ablation ICP-MS analyses

Foraminiferal specimens were individually cleaned using 400 µl oxidative reagent (1:1 30% H_2O_2 and 0.1M NaOH) in a water bath (65°C) for four 2.5-minute intervals (c.f., Westgård et al., 2026; Barker et al., 2003). The reagent was then removed, and specimens rinsed 3 times in ~1mL 18.2 MΩcm MilliQ-water. Specimens were mounted on glass slides using double-sided cellulose tape prior to laser ablation.

The final 2–4 chambers of the shell whorl were analysed using a spot size of 30 µm at 10% intensity with an energy density of 0.8 mJ/cm^2 and a repetition rate of 5 Hz. The dwell time for analysis was 40 seconds for thinner, non-crusted shells and 60 seconds for thicker, crusted shells (c.f., Westgård et al., 2026). Every ~100 ablations were bracketed by analysis of reference materials NIST SRM 610, NIST SRM 612 (measured at 20% intensity), pressed carbonate powder pellets of JCp-1 (*porites sp.*, GSJ, Okai et al., 2002) and JCt-1 (*Tridacna gigas,* GSJ, Inoue et al., 2004), and USGS MACS-3 carbonate pellet (Jochum et al., 2005). Ablations were followed by a 30-second wash out. This study is based on ^{24}Mg, ^{43}Ca, ^{135}Ba, and ^{138}Ba.

2.5 Data processing and analysis

Exported time resolved data in counts per second were processed using iolite 4 (Paton et al., 2011; Paul et al., 2023). Raw element data were normalised to ^{44}Ca and then calibrated using NIST610, NIST612 and JCp-1. JCt-1 and MACS-3 were analysed as unknowns for quality control. Mg/Ca is within <10% of reference values for JCt-1 (2022), and within <20% for MACS-3 (2021, and 2022, c.f., Westgård et al., 2026).

Further data processing and analysis were performed in R (Rcoreteam, 2022). Laboratory-grown calcite was identified, and crust and lamellar calcite were distinguished using open source code LabGrown and IDCrust developed by Westgård et al. (2026) (https://github.com/Adele-W/Westgard-et-al.-2025). In this study, data is presented for the laboratory-grown shells in three categories: crust (CC), lamellar calcite (LC), and both components combined (CC + LC). Not all laboratory-grown chambers were encrusted, and in some chambers, there was laboratory-grown crust on top of ocean-grown lamellar

https://doi.org/10.5194/egusphere-2026-2415
Preprint. Discussion started: 6 May 2026
© Author(s) 2026. CC BY 4.0 License.

calcite. The category for both components (CC + LC) therefore only include shells where both components were present and grown under laboratory conditions. Shell thickness was estimated based on length of the shell profile and ablation rate (0.4 µm/sec, c.f., Westgård et al., 2026). The crust thickness (proportion as % of total shell thickness) was estimated using the length of the shell profile and the crust-lamellar boundary (breakpoint) identified by IDCrust.

Distribution coefficients D_{Mg} were calculated for each water treatment (Table 3) according to equation 1, e.g., Branson et al. (2025).

$$D_{element} = \frac{element/Ca_{calcite}}{element/Ca_{seawater}} \quad (1)$$

Scatterplots exploring co-variance of water treatments, environmental conditions and Mg/Ca, as well as regression lines for Mg/Ca relationships with environmental conditions were plotted and modelled using R. The best fit model produced in R also provides statistical test parameters for Pearsons R, standard error, t-test, and p-values where relevant. Pseudo-R^2 for non-linear relationships were calculated using the residual sum of squares divided by the total sum of squares. The environmental relationships are presented in three ways: 1) Mg/Ca ratios for all ablated chambers; 2) the median Mg/Ca in each water treatment; and 3) the distribution coefficients.

3 Results

3.1 Environmental influence on crust formation

The total number of laboratory-grown chambers was 525 and the number of crusted chambers is 279 (Table S3). We observe crust growth in all treatments; the pH 8.15 treatment without co-varying carbonate ion had the lowest number of crusted chambers (21% of measured chambers, Table 3 & S3), while all chambers were crusted in the high salinity (36.7) treatment from evaporated seawater and the salinity 33.6 treatment. From the 525 analysed laboratory-grown chambers, in 154 chambers only crust was identified from the LabGrown & IDCrust algorithms, suggesting these chambers were characterized by laboratory grown crust that was added onto ocean grown lamellae, that the chamber wall was not

https://doi.org/10.5194/egusphere-2026-2415
Preprint. Discussion started: 6 May 2026
© Author(s) 2026. CC BY 4.0 License.

ablated through, or alternatively they consisted of predominantly crust. Based on tests were both crust and lamellar calcite was analysed (and laboratory-grown), we observe that the total shell thickness decreases with decreasing pH and temperature ($|R|>0.5$, $p>0.05$). We also observe decreased total shell thickness with increasing [$CO3^{2-}$] ($R= -0.8$, $p>0.05$). There is no statistically significant change in total shell thickness with changing salinity. We observe significantly lower proportions of crust in the shell at higher salinities compared to low salinities ($R= -0.7$, $p<0.05$). We also observe a decrease in the proportion of crust with decreasing pH and/or [CO_3^{2-}], and higher temperatures ($|R|>0.5$, $p>0.05$, Fig. 1).

https://doi.org/10.5194/egusphere-2026-2415
Preprint. Discussion started: 6 May 2026
© Author(s) 2026. CC BY 4.0 License.

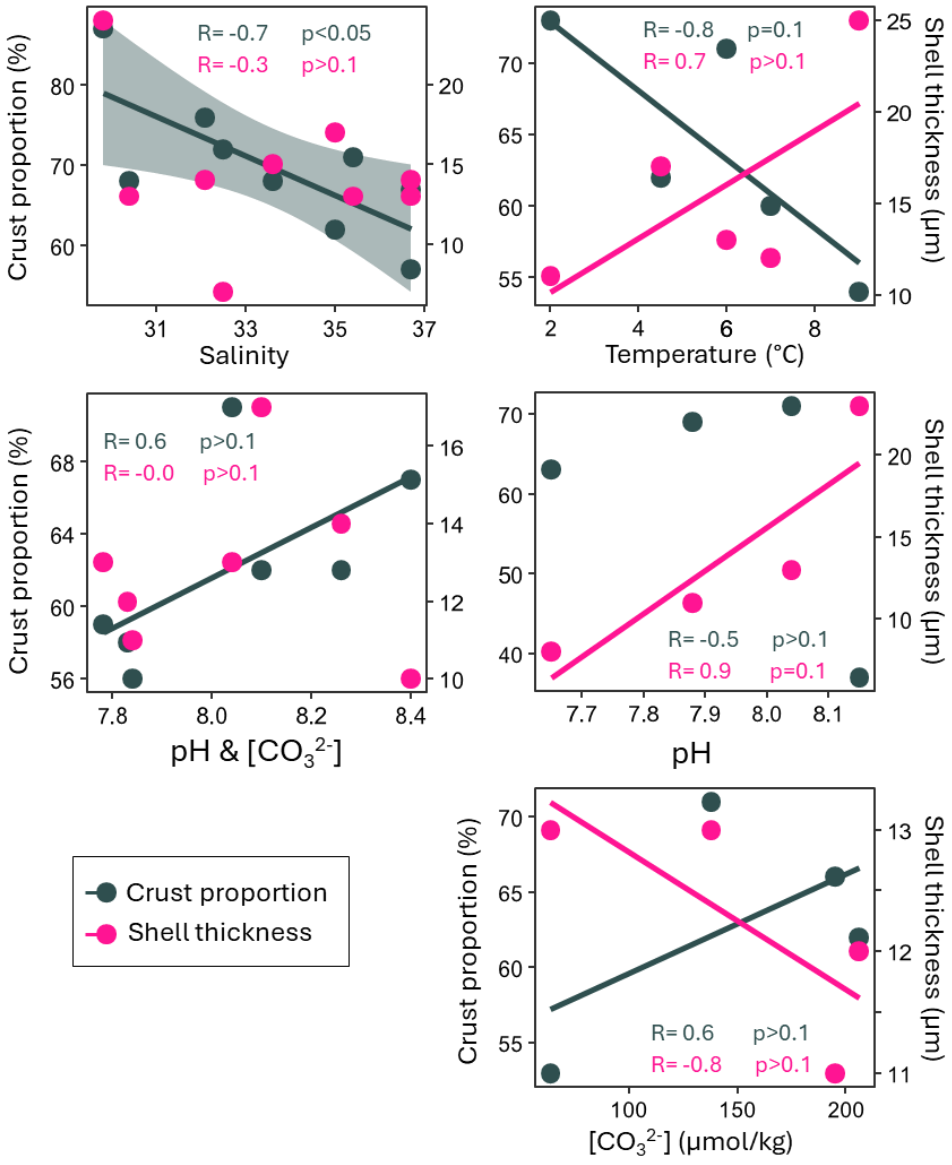

285

286 *Figure 1. Mean crust proportion (as % of total shell thickness) and total shell thickness (µm) in each*
287 *water treatment correlated with environmental conditions. The plot includes only specimens where both*
288 *the crust and lamellae were laboratory-grown. Trend lines are included for relationships where |R|>0.5.*
289 *Significant relationships have a 95% confidence envelope in green shading. See corresponding data in*
290 *table 3 & S3.*

291

https://doi.org/10.5194/egusphere-2026-2415
Preprint. Discussion started: 6 May 2026
© Author(s) 2026. CC BY 4.0 License.

3.2 Culture media and Distribution coefficients

The conditions and elemental composition of culture media is presented in Tables 2 and S1. Some salinity and pH with co-varying [CO_3^{2-}] experiments were therefore carried out at different temperatures (4.5 or 6°C). We observe minimal difference in seawater Mg/Ca between the two experimental years (5084±549 and 5024±107 mmol/mol in 2021 and 2022 respectively; Table S2) and higher seawater Mg/Ca in culture media compared to natural seawater (4788±102 mmol/mol) from the 2021 collection site.

https://doi.org/10.5194/egusphere-2026-2415
Preprint. Discussion started: 6 May 2026
© Author(s) 2026. CC BY 4.0 License.

Table 3. Median Mg/Ca (mmol/mol), Distribution coefficients (D_{Mg}) for element ratios in seawater treatments to foraminiferal calcite, and shell structure per water treatment. For each Mg/Ca and D_{Mg} crust (CC), lamellar calcite (LC), and both components combined (CC+LC) are listed separately. 36-f and 36-e were prepared using rejection brine and evaporated seawater respectively.

Water treatment		Mg/Ca (mmol/mol)			$D_{Mg/Ca}$ *1000			Shell wall (µm)	%crust (when both CC & LC present)
		CC+LC	CC	LC	CC+LC	CC	LC		
Temperature (ºC)	2	1.4 ±0.29	1.55 ±0.32	1.41 ±0.59	0.30	0.33	0.30	11	73
	4.5	1.28 ±0.64	1.28 ±0.59	2.04 ±1.09	0.27	0.27	0.43	17	62
	6	3.22 ±1.22	2.18 ±0.95	2.73 ±1.99	0.63	0.43	0.53	13	71
	7	1.62 ±0.14	1.77 ±0.36	1.95 ±0.56	0.34	0.37	0.41	12	60
	9	2.68 ±0.60	4.97 ±1.24	4.50 ±2.36	0.52	0.97	0.88	25	54
Salinity	29.8	1.94	1.60 ±0.17	2.09 ±0.51	0.37	0.31	0.4	24	87
	30.4	1.90 ±1.53	2.65 ±1.29	4.23 ±1.59	0.38	0.53	0.85	13	68
	32.1	1.99	1.81 ±0.06	2.19 ±0.69	0.38	0.35	0.42	14	76
	32.5	2.36 ±0.94	2.8 ±1.39	2.34 ±2.38	0.49	0.58	0.49	7	72
	33.6	1.74 ±0.51	1.68 ±0.63	2.03 ±0.31	0.33	0.32	0.39	15	68
	36.7-f	4.40 ±0.43	4.38 ±1.19	3.89 ±1.40	0.84	0.83	0.74	13	67
	36.7-e	1.98 ±0.14	1.67 ±0.29	2.30 ±0.17	0.38	0.32	0.44	14	57
pH and carbonate ion (pH total scale)	7.78	3.65 ±1.42	3.86 ±1.45	4.73 ±3.00	0.73	0.77	0.95	13	59
	7.83	2.93 ±1.32	2.48 ±1.32	3.27 ±1.91	0.57	0.48	0.64	12	58
	7.84	3.65	3.97 ±1.05	2.10 ±0.51	0.70	0.77	0.41	11	56
	8.26	1.54 ±0.64	1.55 ±0.81	1.79 ±0.70	0.30	0.30	0.34	14	62
	8.4	1.18	1.35 ±0.1	1.52 ±0.38	0.22	0.25	0.28	10	67
Carbonate ion (µmol/kg)	64	2.31	2.13 ±0.49	2.33 ±0.91	0.46	0.43	0.47	13	53
	195	4.73 ±1.37	3.19 ±1.56	3.44 ±1.55	0.92	0.62	0.67	11	66
	206	3.24 ±1.66	3.41 ±1.53	3.59 ±3.12	0.65	0.69	0.72	12	62
pH (decoulped carbonate ion)	7.65	6.59	4.26 ±1.73	8.65 ±2.64	1.33	0.86	1.75	8	63
	7.88	5.23 ±1.52	4.38 ±1.92	7.15 ±4.54	1.06	0.88	1.44	11	69
	8.15	2.15 ±0.34	1.91 ±0.58	2.23 ±0.36	0.44	0.39	0.45	23	37

https://doi.org/10.5194/egusphere-2026-2415
Preprint. Discussion started: 6 May 2026
© Author(s) 2026. CC BY 4.0 License.

3.3 Temperature

Mg/Ca has a significant positive exponential relationship ($p<0.005$) with temperature in both the crust and lamellar calcite when all chambers are included (Fig. 2). Although R^2 may not be accurately representative for non-linear relationships, pseudo-R^2 was calculated to 0.5 and 0.2 in the crust and lamellar calcite respectively (Table 4). The pseudo-R^2 for both components combined is 0.3 with $p<0.005$. The exponential curve is significantly steeper for the crust than lamellar calcite and the two curves therefore converge at higher temperatures (>9°C). The relationship is also significant in the crust treatment medians and both the crust and lamellae distribution coefficients.

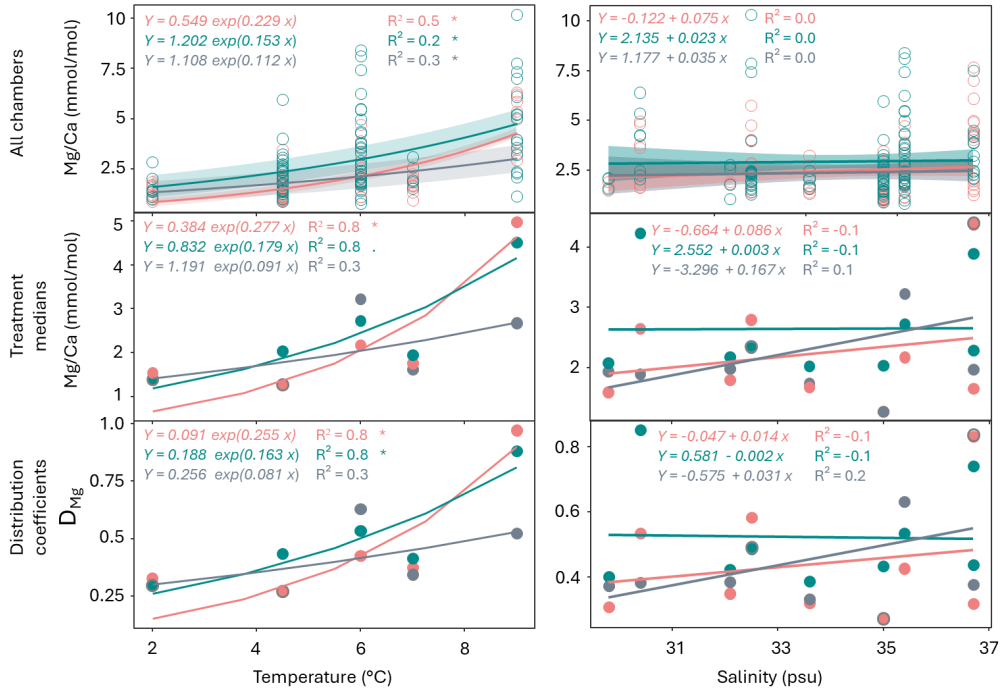

*Figure 2. Element/Ca vs temperature (left) and salinity (right) regression lines with all chambers included (left), treatment medians (middle), and distribution coefficients (right). Pink line = crust, green line = lamellae, grey line = both combined. Statistical significance: *p<0.05, .p<0.1.*

3.4 Salinity

https://doi.org/10.5194/egusphere-2026-2415
Preprint. Discussion started: 6 May 2026
© Author(s) 2026. CC BY 4.0 License.

There is a weak positive relationship between Mg/Ca and salinity, however this is not significant ($p>0.1$, Fig. 2). Due to the methods used to modify the seawater salinity, DIC, [HCO_3^-], and total alkalinity (TA) co-varied linearly with salinity (Table 2), [CO_3^{2-}] also varied between the salinity treatments, however not linearly.

3.5 Carbonate chemistry

The three carbonate chemistry treatments (pH & [CO_3^{2-}], pH, and [CO_3^{2-}]) all have significant influence on Mg/Ca in the crust, lamellae and both components combined (Table 4, Fig. 3). There is a significant negative correlation between Mg/Ca and pH (Fig. 3 left and middle panels). This relationship is steeper (~4.7 compared to ~7.3 mmol/mol decrease in Mg/Ca per pH unit based on crust in all chambers) when [CO_3^{2-}] does not co-vary with pH. The pH with co-varying [CO_3^{2-}] (typical in nature) relationship with Mg/Ca is significant for all chambers, treatment medians, and the distribution coefficients (Fig. 3 left panel). When the two parameters do not co-vary, the relationship is not significant in the crust when using treatment medians and distribution coefficients (Fig. 3 middle panel). There are significant positive relationships between Mg/Ca and [CO_3^{2-}] in the crust and lamellar calcite, but not the two components combined (Fig. 3 right panel). When using treatment medians and distribution coefficients the Mg/Ca–[CO_3^{2-}] relationship is only significant in the lamellae. A plot of Mg/Ca correlated to pH with co-varying [CO_3^{2-}] with treatments performed at 6°C normalised to 4.5° using the temperature relationships for crust, lamellar calcite, and both components separately (section 3.3) is shown in Fig. S2 (Table S4).

https://doi.org/10.5194/egusphere-2026-2415
Preprint. Discussion started: 6 May 2026
© Author(s) 2026. CC BY 4.0 License.

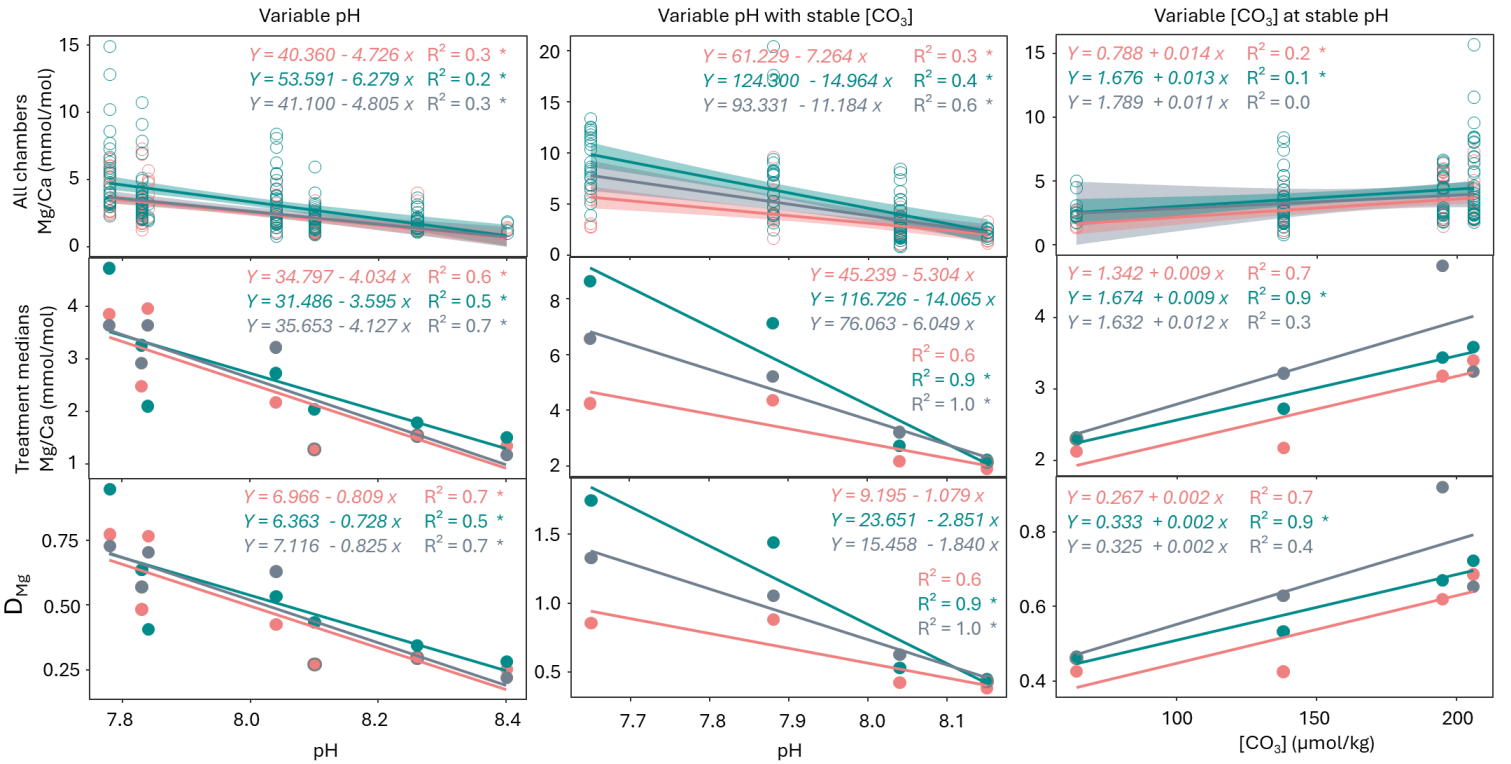

339

340 *Figure 3. Regression lines for the Mg/Ca relationship with carbonate chemistry parameters. Mg/Ca (mmol/mol) for all chambers (top), Mg/Ca treatment medians*
341 *(middle), and Partitioning coefficients (D_{Mg}, bottom). Pink line = crust, green line = lamellae, grey line = both combined. Statistical significance: *p<0.05,*
342 *.p<0.1. See also Fig. S2.*

343

https://doi.org/10.5194/egusphere-2026-2415
Preprint. Discussion started: 6 May 2026
© Author(s) 2026. CC BY 4.0 License.

Table 4. Calibration equations, R^2, and p-values for Mg/Ca relationship with temperature and carbonate chemistry in crust, lamellar calcite, and both components with all chambers included, treatment medians, and distribution coefficients (D_{Mg}). Only significant relationships are included.

Mg/Ca relationship	Data type	Crust calcite:	Lamellar calcite:	Both components:
Mg/Ca temperature	All chambers	Mg/Ca = 0.549±0.099 exp (0.229±0.024 T) R^2 = 0.5 p = 4.45 *10^{-14}	Mg/Ca = 1.202±0.263 exp (0.153±0.031 T) R^2 = 0.2 p = 2.69 *10^{-6}	Mg/Ca = 1.108±0.249 exp (0.112±0.035 T) R^2 = 0.3 p = 0.003
	Treatment medians	Mg/Ca = 0.384±0.259 exp (0.277±0.084 T) R^2 = 0.5 p = 0.05		
	Distribution coefficients	Mg/Ca = 0.091±0.056 exp (0.255±0.078 T) R^2 = 0.8 p = 0.05	Mg/Ca = 1.202±0.068 exp (0.153±0.050 T) R^2 = 0.8 p = 0.05	
Mg/Ca pH with co-varying [CO_3^{2-}]	All chambers	Mg/Ca = 40.360 - 4.726 pH R^2 = 0.3 p = 7.6 *10^{-12}	Mg/Ca = 53.591 - 6.279 pH R^2 = 0.2 p = 1.4 *10^{-10}	Mg/Ca = 41.100 - 4.805 pH R^2 = 0.3 p = 2.5 *10^{-7}
	Treatment medians	Mg/Ca = 34.797 - 4.034 pH R^2 = 0.6 p = 0.02	Mg/Ca = 31.486 – 3.595 pH R^2 = 0.5 p = 0.05	Mg/Ca = 35.653 - 4.127 pH R^2 = 0.7 p = 0.01
	Distribution coefficients	Mg/Ca = 6.966 – 0.809 pH R^2 = 0.7 p = 0.01	Mg/Ca = 6.363 – 0.728 pH R^2 = 0.5 p = 0.05	Mg/Ca = 7.116 – 0.825 pH R^2 = 0.7 p = 0.01
Mg/Ca pH without co-varying [CO_3^{2-}]	All chambers	Mg/Ca = 61.229 – 7.264 pH R^2 = 0.3 p = 1.9 *10^{-5}	Mg/Ca = 124.300 - 14.964 pH R^2 = 0.4 p = 3.5 *10^{-11}	Mg/Ca = 93.331 - 11.184 pH R^2 = 0.6 p = 1.3 *10^{-5}
	Treatment medians		Mg/Ca = 116.726 – 14.065 pH R^2 = 0.9 p = 0.04	Mg/Ca = 76.063 – 6.049 pH R^2 = 1.0 p = 0.01
	Distribution coefficients		Mg/Ca = 23.651 – 2.851 pH R^2 = 0.9 p = 0.05	Mg/Ca = 15.458 – 1.840 pH R^2 = 1.0 p =0.01
Mg/Ca [CO_3^{2-}] without co-varying pH	All chambers	Mg/Ca = 0.788 + 0.014[CO_3^{2-}] R^2 = 0.2 p = 4.3 *10^{-4}	Mg/Ca = 1.676 + 0.013 [CO_3^{2-}] R^2 = 0.1 p = 0.006	
	Treatment medians		Mg/Ca = 1.342 + 0.009 [CO_3^{2-}] R^2 = 0.9 p = 4.4 *10^{-12}	
	Distribution coefficients		Mg/Ca = 0.325 + 0.002 [CO_3^{2-}] R^2 = 0.9 p = 0.04	

https://doi.org/10.5194/egusphere-2026-2415
Preprint. Discussion started: 6 May 2026
© Author(s) 2026. CC BY 4.0 License.

4 Discussion

4.1 New Mg/Ca-temperature calibrations for the crust and lamellar calcite

The Mg/Ca-temperature relationship presented in this study substantially extends the culture-based calibration range in this species from 9–12°C (c.f., Davis et al., 2017) to 2–7°C. While both the crust and lamellar calcite have significant exponential Mg/Ca relationships with temperature, the Mg/Ca is consistently lower in the crust than lamellar calcite at all temperatures. However, as shown in Westgård et al. (2026), but confirmed here over a greater range of temperatures, the difference between the crust and lamellae decreases with increasing temperature from ~23% higher Mg/Ca in the lamellae at 4.5°C (largest difference) to 5% lower Mg/Ca in the lamellae at 9°C when comparing treatment medians. The exponential curve for the crust is therefore steeper than for the lamellar calcite and thus, the calibration curves converge at ~8°C using the treatment medians and or >9°C using all chambers (Fig. 2, 4). As the habitat of *N. pachyderma* includes temperatures from <0 to >10°C, its use in palaeoreconstructions also covers a wide range of temperatures. Therefore, temperatures obtained from the crust and lamellar calcite will be appreciably different depending on the specimen's growth temperatures in most of this temperature range.

The steepness of the combined crust and lamellar calibration curve is strongly influenced by crust:lamellae proportions as a larger proportion of crust will shift the specimen median value towards the crust values or towards the lamellar median if the lamellar calcite is proportionally thicker. This also introduces more variability and "noise" to the combined calibration curve. In addition, as we observe proportionally less crust at higher temperatures (Fig. 1), calibrations based on both components are then disproportionally influenced by lamellar values with increasing temperature with the overall effect of decreasing temperature sensitivity (Fig. 4). As crust thickness varies with environmental conditions and downcore in marine sediments, i.e., through time, this further complicates the application of whole-specimen Mg/Ca-based temperature estimates from this species. We therefore reaffirm the need to consider the two components separately in development and application of proxies in this species (Jonkers et al., 2016; Davis et al., 2017; Livsey et al., 2020; Westgård et al., 2026). We thus recommend

https://doi.org/10.5194/egusphere-2026-2415
Preprint. Discussion started: 6 May 2026
© Author(s) 2026. CC BY 4.0 License.

using the calibration curves presented in this study for each component separately, which include the first crust-only calibration.

The Mg/Ca values we obtain are largely comparable with previous culture and plankton-tow based studies (i.e., Davis et al., 2017; Livsey et al., 2020) at equivalent temperatures (Fig. 4, panel B). The lamellar calcite Mg/Ca-temperature calibration by Livsey et al. (2020) using *N. pachyderma* sampled by plankton tow is similar to the lamellar curve obtained in this study, although their absolute values are higher than our observations at the lower temperature range (<4°C). Thus by compiling the treatment medians from this study, with the data from Davis et al. (2017) and the means from Livsey et al. (2020) we present an extended calibration for the lamellar calcite (Fig 4, panel B). A comparable compilation cannot be produced for the crust as such data is not published outside of this study.

The Mg/Ca values reported in this study, along with those from other studies analysed by LA-based methods (e.g., Davis et al., 2017; Livsey et al., 2020) are higher than Mg/Ca values from sediment trap and core top samples at equivalent temperatures analysed by solution-based approaches (Fig. 4, e.g., Jonkers et al., 2016; Kozdon et al., 2009a; Morley et al., 2024). This difference may partly reflect variation in crust proportions, sample preservation, and potential loss of lamellar calcite during sample handling for solution-based analyses (c.f., Westgård et al., 2026). Additional sources of uncertainty include the estimation of true water temperatures for core-top samples, as growth temperatures can only be approximated, and differences in single- versus multi-specimen cleaning procedures, which can affect measured Mg/Ca values (Lee et al., 2025).

https://doi.org/10.5194/egusphere-2026-2415
Preprint. Discussion started: 6 May 2026
© Author(s) 2026. CC BY 4.0 License.

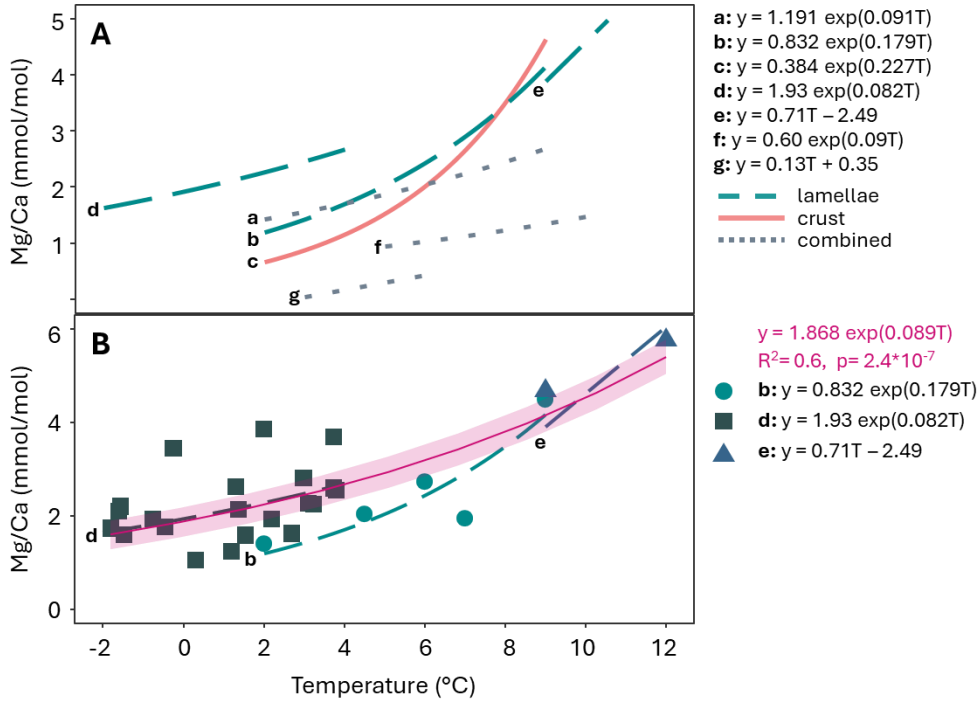

*Figure 4. Mg/Ca-temperature equations from this study plotted alongside published equations. A) Equations based on crust, lamellae, or both combined are indicated by colours pink, green, and grey respectively. a, b, c = This study, d = Livsey et al. (2020), e = Davis et al. (2017), f = Jonkers et al. (2013), and g = Kozdon et al. (2009a). Calibrations by Davis et al. (2017), and Livsey et al. (2020), are both based on lamellar calcite only and analysed by LA-ICP-MS. Calibrations by Jonkers et al. (2013) and Kozdon et al. (2009a), are based on wholeshell analysis by solution of crusted samples from sediment trap and core top respectively. B) Compilation of data and calibrations based on the lamellar calcite only with a combined lamellar calibration curve (R^2= 0.6, p= 2.4*10^{-7}).*

4.2 Carbonate chemistry and salinity influences on Mg/Ca

We observe significant carbonate chemistry influence on Mg/Ca, with opposite effects from pH (negative) and [CO_3^{2-}] (positive) on both crust and lamellar calcite (Fig. 3, Table 4). When the two carbonate system parameters are decoupled, the negative Mg/Ca relationship with pH produces a steeper slope than the positive slope of [CO_3^{2-}]. This suggests pH exerts a stronger control on Mg/Ca than [CO_3^{2-}].

This finding is in contrast to Davis et al. (2017) who observed no significant pH and/or [CO_3^{2-}] (co-varied) influence on Mg/Ca in the closely related species, *Neogloboquadrina incompta*. Other studies

https://doi.org/10.5194/egusphere-2026-2415
Preprint. Discussion started: 6 May 2026
© Author(s) 2026. CC BY 4.0 License.

(Morley et al., 2024; Lea et al., 1999; Russell et al., 2004; Evans et al., 2018) have reported significant carbonate chemistry influence on Mg/Ca however none of these decoupled pH from [CO_3^{2-}] and/or [HCO_3^-] although Evans et al. (2018) decoupled pH and DIC. Some studies such as Morley et al. (2024) on *N. pachyderma* and Russell et al. (2004); Allen et al. (2016) on multiple warm water species observed a negative exponential relationship between Mg/Ca and seawater [CO_3^{2-}]. However, in these studies, pH and [CO_3^{2-}] likely co-vary (as is typical in nature) and thus the driving parameter could not be isolated. Allen et al. (2016) also observed increased Mg/Ca with [CO_3^{2-}] when pH was kept constant in *Trilobatus sacculifer* (R=0.96, p=0.04) while it decreased when pH and [CO_3^{2-}] co-varied, in line with our results on *N. pachyderma*. We also obtain a significant negative Mg/Ca relationship with [CO_3^{2-}] (and pH, Fig. S3) in the pH treatment with co-varying [CO_3^{2-}]. This Mg/Ca-[CO_3^{2-}] relationship is comparable that to observed by Morley et al. (2024), with an overall decrease from ~5 to ~1 mmol/mol Mg/Ca over ~70-240 µmol/kg [CO_3^{2-}] (or pH 7.7-8.4 in our study, Fig. S3). However, we observe a negative relationship between Mg/Ca and pH at "constant" [CO_3^{2-}] (Fig. 3) and a positive relationship with [CO_3^{2-}] at "constant" pH (Fig. S3). Thus, the negative relationships and Russell et al. (2004); Allen et al. (2016); Morley et al. (2024) observed likely also represent a negative relationship to pH (with co-varying [CO_3^{2-}]) rather than to [CO_3^{2-}].

We observed a positive Mg/Ca sensitivity to salinity (~9% and ~0.3% per salinity unit in crust and lamellae respectively) comparable to other studies (3-5 %, e.g., Allen et al., 2016; Hönisch et al., 2013). However, the Mg/Ca-salinity relationships in this study was not statistically significant , in line with Bertlich et al. (2021). In our salinity experiments, carbonate chemistry and temperature were not always fixed (Fig. S1, Table 2). Thus, for any temperature, pH, and [CO_3^{2-}] values that are outside the standard error of the T4.5°C treatment, we used our Mg/Ca-relationships from the temperature and carbonate chemistry experiments (Table 4 & 5) to isolate the salinity effects on Mg/Ca. This results in a steeper positive (~20% and ~10% in crust and lamellae respectively) Mg/Ca-relationship with salinity (Fig. 5, Table S4), however it is also not significant at the 95% confidence interval. As carbonate chemistry often co-varies with salinity in nature (e.g., Olsen et al., 2020), the uncorrected salinity-Mg/Ca relationship (in which carbonate chemistry and salinity covary) may represent the "natural"

https://doi.org/10.5194/egusphere-2026-2415
Preprint. Discussion started: 6 May 2026
© Author(s) 2026. CC BY 4.0 License.

salinity/carbonate chemistry effect in many settings and the pH, [CO_3^{2-}], and salinity-influences on Mg/Ca may therefore effectively cancel each other out. For example, meltwater intrusions leading to concurrent freshening and pH decrease would have opposing impacts on foraminiferal Mg/Ca.

We observed significant differences in Mg/Ca between the two high (36.7) salinity treatments despite all measured environmental parameters being equivalent (e.g., temperature, salinity, pH, and [CO_3^{2-}], Table 2). The two treatments were prepared differently by using rejection brine and evaporated seawater (Section 2.2, and Table 2) and obtained statistically different Mg/Ca (e.g., crust values were 4.38±1.19 and 1.67±0.29 mmol/mol respectively). Although we cannot provide a mechanistic explanation, it is worth noting that there were more laboratory-grown (n=23) and crusted chambers (n=11) in the treatment prepared with rejected brine compared to the treatment made using evaporated seawater (only 6 lab-grown and crusted chambers in total, Table 3). This difference could be caused by random variability or a "vital effect" caused by an unknown, not measured, variable which influences chamber precipitation and Mg/Ca.

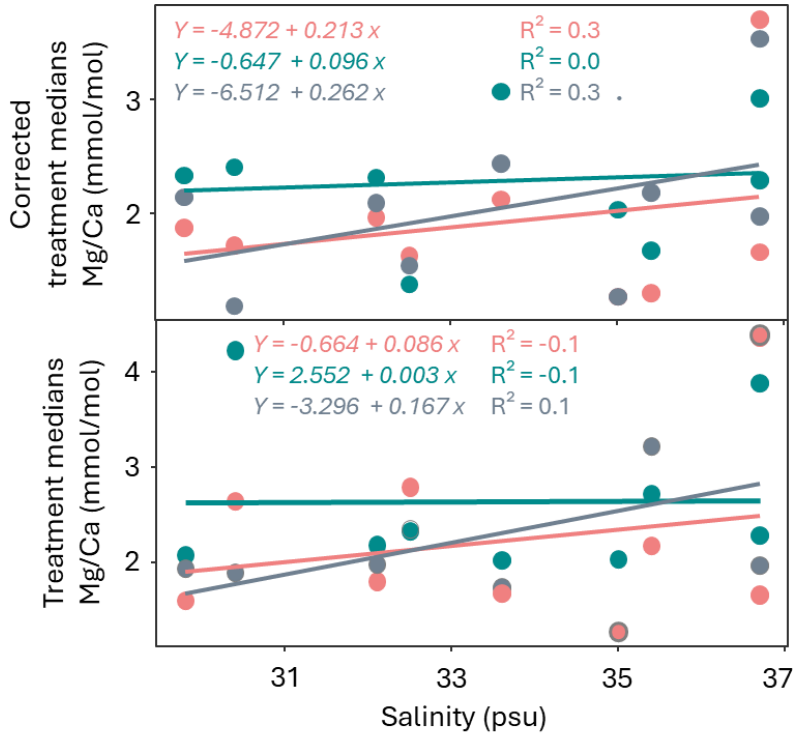

https://doi.org/10.5194/egusphere-2026-2415
Preprint. Discussion started: 6 May 2026
© Author(s) 2026. CC BY 4.0 License.

*Figure 5. The Mg/Ca relationship with salinity when corrected for influence by T, pH and [CO_3^{2-}] (top) and without correction (bottom, also in Fig. 2). Regression lines for Mg/Ca treatment medians (mmol/mol). Pink line = crust, green line = lamellae, grey line = both combined. Statistical significance: *p<0.05, .p<0.1. Note the different y-axes.*

4.3 Crust-lamellae proportions are influenced by environmental conditions

Although crust formation occurred in all treatments, environmental conditions clearly influence the proportion of crust to lamellar calcite. Increasing salinity is significantly correlated with lower crust proportions (Fig. 1, Table 3 & S3). We also observed lower proportion of crust at lower pH, and higher [CO_3^{2-}] and temperatures, though not significantly at the 95% confidence level. Additionally, we observe overall thinner shells at lower pH values. The general reduction of %crust and shell thickness with decreasing pH and [CO_3^{2-}] supports evidence of negative impacts of ocean acidification on shell calcification (c.f., Chaabane et al., 2024; Manno et al., 2012; Anglada-Ortiz et al., 2021). Also, higher temperatures, considered suboptimal for *N. pachyderma* in this region, were also associated with reduced crust proportions, although thicker shells (c.f., Chaabane et al., 2024; Westgård et al., 2023). These results thus indicate that crust and shell thickness is environmentally influenced and suggest processes such as Atlantification (expansion of warm, saline Atlantic water to the Arctic, c.f., Ingvaldsen et al., 2021) and ocean acidification may lead to reduced calcification in the future , with also potential implications for carbon export and ballasting (c.f., Tell et al., 2022; Anglada-Ortiz et al., 2021).

4.4 Proxy calibration and implications for palaeoceanographic reconstructions

The presented Mg/Ca-calibration curves significantly extend the range covered by culture-based calibrations in *N. pachyderma*, from 9–12°C (Davis et al., 2017) to 2–9°C. This has potential to significantly improve temperature-reconstructions in the subpolar and polar regions where SSTs can be as low as -2°C. In addition, we present a compilation calibration including data from Davis et al. (2017)

https://doi.org/10.5194/egusphere-2026-2415
Preprint. Discussion started: 6 May 2026
© Author(s) 2026. CC BY 4.0 License.

and Livsey et al. (2020), resulting in a combined calibration from -2 to 12°C for the lamellar calcite (Fig. 4). However, crust often dominates the shell weight in the fossil record (40-80%, c.f., Westgård et al., 2026; Kozdon et al., 2009a), and some studies report loss of the lamellar calcite during diagenesis, handling, and/or cleaning, the crust calibration may therefore be more important in paleo-reconstructions.

Both the difference in Mg/Ca between the crust and lamellae and the proportion of crust to lamellae vary with environmental conditions, for example both decrease with temperature (Fig 1 & 2). In downcore reconstructions, both aspects are sources of uncertainty. Increasing temperature leads to more influence from the high-Mg/Ca lamellae, skewing temperature-estimates based on whole-shell analysis towards higher temperatures. Therefore, not separating the two components results in inaccuracy and uncertainties in temperature estimates. When both crust and lamellar calcite are present, they can be separated by laser ablation analysis using the methods developed by Westgård et al. (2026) and the corresponding Mg/Ca calibrations presented in this study can be applied to each component, thus reducing the uncertainty introduced by crust-lamellar variations and differences.

Sea ice formation, meltwater input, and river discharge alter the carbonate chemistry and salinity of the adjacent seawater (e.g., Fransson et al., 2013). We show that carbonate chemistry significantly influences Mg/Ca in *N. pachyderma* (section 3.5 & 4.2) and should therefore be considered in paleoclimate reconstructions in polar waters and sites influenced by these processes. However, the pH influence on Mg/Ca appears to be less impactful in the pH range 8.1–8.4 (Fig. 3), which is the expected range in the Quaternary pelagic Nordic Seas (e.g., Ezat et al., 2017), thus we expect limited pH influence on Mg/Ca in this region on such timescales.

4.5 Implications for biomineralisation

The different responses of Mg/Ca in the crust and lamellar calcite to changing environmental parameters suggests they calcify via different biomineralisation mechanisms, supporting previous findings (Westgård et al., 2026). This particularly applies to the Mg/Ca-temperature and -pH relationships where

https://doi.org/10.5194/egusphere-2026-2415
Preprint. Discussion started: 6 May 2026
© Author(s) 2026. CC BY 4.0 License.

the difference between the two components decreases with increasing temperature and pH. Environment also influences the total shell thickness and balance between these two components such that changes in the environment therefore affects crust calcification in two ways: the final proportions of crust to lamellae and the incorporation of trace elements into each component.

In this study Mg/Ca responds oppositely to changing pH and [CO_3^{2-}], and we observe larger differences in steepness of the slope of the relationship between the crust and lamellar calcite in response to pH but not [CO_3^{2-}] (Fig. 3). Increasing [CO_3^{2-}] likely leads to increased calcite precipitation rates, which results in higher D_{Mg} in inorganic precipitation experiments (e.g., Branson et al., 2025; Allen et al., 2016), potentially explaining the positive Mg/Ca correlation with [CO_3^{2-}]. Such an increase can also be explained by Rayleigh fractionation (c.f., Evans et al., 2018 and references therein) if the higher calcification rates occurred from the same sized pool of Ca, where Mg abundance is ~5x higher.

The Mg/Ca-relationship to pH with constant [CO_3^{2-}] results in a steeper negative relationship (with different slopes for the crust and lamellar calcite) compared to changing pH with co-varying [CO_3^{2-}] (where the crust and lamellar calcite have relatively similar slopes), in-line with removal of a "[CO_3^{2-}]-effect" on Mg/Ca. This suggests that there is a different driver behind the Mg/Ca response to pH than the Mg/Ca response to [CO_3^{2-}]. We suggest that the Mg/Ca response to [CO_3^{2-}] may be driven by calcification rate (a physical process), but that the response to pH and the observed differences between the crust and lamellar calcite may instead be driven by a physiological process. In particular, foraminifera are thought to have a high pH-calcification fluid to aid calcification regulated by H^+-pumping (De Nooijer et al., 2009; Toyofuku et al., 2017). The low pH culture media would require the specimen to increase the pH of its internal calcifying fluid more than at higher pH, at a higher energy-cost (e.g., Morley et al., 2024; François et al., 2025; De Nooijer et al., 2009). This would leave less energy available for Mg-removal from the site of calcification to counter the inhibiting effect Mg^{2+} has on calcification (e.g., Zeebe and Sanyal, 2002; Jacob et al., 2017; De Nooijer et al., 2014; Westgård et al., 2026), thus providing an explanation for the observed lower Mg/Ca ratios at lower pH (c.f., Evans et al., 2018). This is also reflected in the thinner shells with a lower proportion of crust observed at lower pH. Alternatively, the pH-effect on Mg/Ca could be explained if proton-removal via the enzyme Ca-

https://doi.org/10.5194/egusphere-2026-2415
Preprint. Discussion started: 6 May 2026
© Author(s) 2026. CC BY 4.0 License.

ATPase (e.g., Toyofuku et al., 2017) is less efficient at lower pH (e.g., Guo and Messer, 1978), thus also transporting less Ca^{2+} at lower pH, resulting in higher Mg/Ca. Assuming *N. pachyderma* modulates the pH of its calcifying fluid, high Mg/Ca at low pH does not align with recent findings for benthic foraminifera (François et al., 2025) suggesting greater difference between seawater pH and the calcification site is correlated with higher Ca^{2+} flux, as this would lead to lower Mg/Ca at lower pH which is the opposite of what we observe (Fig. 3). This may imply that in planktic and benthic foraminifera biomineralisation influences Mg/Ca in contrasting ways.

5 Conclusions

We present a range of laboratory-based investigations into the variability of Mg/Ca in *Neogloboquadrina pachyderma* to a range of realistic past and future polar environmental parameters including temperature, salinity, and carbonate chemistry with decoupled pH and $[CO_3^{2-}]$. We observe that the proportion of crust in the shell in part is controlled by environmental conditions and decreases significantly with increasing salinity, and not significantly with decreasing pH and $[CO_3^{2-}]$ and increasing temperature. The total shell thickness also decreases with decreasing pH with implications for downcore reconstructions, and foraminifera ecology and carbon export in relation to ongoing climate change.

Using LA-ICP-MS and open-source code (Westgård et al., 2026) we were able to separate the geochemical signals of crust and lamellar calcite, and observed significant differences in the two components' Mg/Ca-sensitivity to environmental conditions (based on 525 lab-grown chambers, Table S3). The new low-temperature Mg/Ca-temperature calibrations for *N. pachyderma* for the crust ($Mg/Ca = 0.549 \pm 0.099 \exp^{(0.229 \pm 0.024T)}$) and lamellar calcite ($Mg/Ca = 1.202 \pm 0.263 \exp^{(0.153 \pm 0.031T)}$) significantly extend the lower temperature range (from 9°C to 2°C) of culture-based Mg/Ca-calibrations. By uncoupling the carbonate system parameters, we find that pH has significant negative influence and $[CO_3^{2-}]$ has significant positive influence on Mg/Ca. When the two parameters co-vary, pH is the primary driver of the relationship, causing a decrease in Mg/Ca with increasing pH & $[CO_3^{2-}$

https://doi.org/10.5194/egusphere-2026-2415
Preprint. Discussion started: 6 May 2026
© Author(s) 2026. CC BY 4.0 License.

554]. This impacts the interpretation of the Mg/Ca-proxy, particularly in regions subject to carbonate
555 chemistry changes, e.g., areas with sea-ice and meltwater input.

556 Separate proxy-calibrations for the crust and lamellar calcite therefore have the potential to significantly
557 reduce inaccuracies and uncertainty of polar palaeoreconstructions using *N. pachyderma* by accounting
558 for changes in crust-lamellar proportions downcore and their different sensitivity to environmental
559 conditions. Thanks to established analytical protocol by Westgård et al. (2026), the suggested separation
560 of shell component is time efficient and does not decrease data quality.

561 We suggest that the positive relationship we observe between Mg/Ca and $[CO_3^{2-}]$ reflects the influence
562 of increased precipitation rate at higher $[CO_3^{2-}]$ on D_{Mg}, as is observed in inorganic experiments (e.g.,
563 Branson et al., 2025 and references therein). Meanwhile the negative Mg/Ca-relationship with pH is
564 likely a physiological response, either driven by: i) less effective transport by Ca-ATPase at lower pH
565 or ii) due to the increased energetic cost of the enhanced levels of proton-pumping needed to elevate
566 calcifying fluid pH at lower seawater pH and the resulting reduction in energy available for Mg^{2+}
567 removal. This is supported by the observed thinner shells with lower crust% at lower pH.

568

https://doi.org/10.5194/egusphere-2026-2415
Preprint. Discussion started: 6 May 2026
© Author(s) 2026. CC BY 4.0 License.

Data availability

Associated data is uploaded to the open repository DataverseNO and a DOI will be provided upon article acceptance.

Supplementary Material

Supplementary material includes figures S1, S2, and S3 showing correlations of culture media parameters, temperature-normalised Mg/Ca (mmol/mol) correlated to pH with co-varying [CO32-], and decoupling of the Mg/Ca-carbonate chemistry relationships. Table S1 gives an overview of published results from each culture experiment. Table S2 shows Mg/Ca_{sw} in mmol/mol of culture media. Table S3 shows the number of *N. pachyderma* chambers grown in culture per treatment, the number of specimens with crust or lamellae only analysed, with both components analysed, and the total number of chambers that grew crust in the lab. Table S4. Lists the corrected Mg/Ca (mmol/mol) treatment medians corresponding to Fig. 5 and S2.

Author contributions

The study was designed by MME, AW, JM, GLF. AW, JM, MME, TC, and FS contributed to sample collection and culturing. AW, GLF, and AM analysed the foraminifera samples, and MC analysed water samples. MME contributed with finances and original research plan. AW wrote the first article draft, and all authors contributed to the article and approved the version included in the thesis.

Competing interests

The authors declare no competing interests.

Acknowledgements

We thank the captains and crews of RV Helmer Hanssen and the UiT cruise- and laboratory-engineers; Truls Holm, Karina Monsen, Ingvild Hald, Trine Dahl, Bjørn Runar Olsen and Matteus Lindgren for their support with sampling and laboratory-work. We also thank Naima El bani Altuna, Christine Lockwood-Ireland, Franziska Tell, Elwyn de la Vega, and Pushpak Martin for their support during

https://doi.org/10.5194/egusphere-2026-2415
Preprint. Discussion started: 6 May 2026
© Author(s) 2026. CC BY 4.0 License.

cruises and culturing. We thank Chris Standish, Matt Cooper and Alex Searle-Barnes at the University of Southampton/NOC for analysing water samples and support with LA-ICP-MS analysis and Helene Lødemel at the Institute of Marine Research for analysing carbonate chemistry water samples. We also thank Nele Meckler and Jeroen Groeneveld for valuable discussions related to this study.

Funding

This study is funded through the ARCLIM project by the Tromsø Research Foundation (project number A31720). This research is also part of the iC3: Centre for ice, Cryosphere, Carbon and Climate, project number 332635 and the ERC synergy project i2B into the Blue, grant number 101118519. T.B.C was supported by the ARCLIM project and ERC StG ForCry, grant number 101040461. GLF was supported by NERC grant NE/W009552/1.

https://doi.org/10.5194/egusphere-2026-2415
Preprint. Discussion started: 6 May 2026
© Author(s) 2026. CC BY 4.0 License.

References

Allen, K. A., Hönisch, B., Eggins, S. M., Haynes, L. L., Rosenthal, Y., and Yu, J.: Trace element proxies for surface ocean conditions: A synthesis of culture calibrations with planktic foraminifera, Geochimica et Cosmochimica Acta, 193, 197–221, 10.1016/j.gca.2016.08.015, 2016.

AMAP: AMAP Assessment 2018: Arctic Ocean Acidification., 2018.

Anand, P., Elderfield, H., and Conte, M. H.: Calibration of Mg/Ca thermometry in planktonic foraminifera from a sediment trap time series, Paleoceanography, 18, n/a–n/a, 10.1029/2002pa000846, 2003.

Anglada-Ortiz, G., Meilland, J., Ziveri, P., Chierici, M., Fransson, A., Jones, E., and Rasmussen, T. L.: Seasonality of marine calcifiers in the northern Barents Sea: Spatiotemporal distribution of planktonic foraminifers and shelled pteropods and their contribution to carbon dynamics, Progress in Oceanography, 218, 103121, https://doi.org/10.1016/j.pocean.2023.103121, 2023.

Anglada-Ortiz, G., Zamelczyk, K., Meilland, J., Ziveri, P., Chierici, M., Fransson, A., and Rasmussen, T. L.: Planktic Foraminiferal and Pteropod Contributions to Carbon Dynamics in the Arctic Ocean (North Svalbard Margin), Frontiers in Marine Science, Volume 8 - 2021, 10.3389/fmars.2021.661158, 2021.

Barker, S., Greaves, M., and Elderfield, H.: A study of cleaning procedures used for foraminiferal Mg/Ca paleothermometry, Geochemistry, Geophysics, Geosystems, 4, https://doi.org/10.1029/2003GC000559, 2003.

Bertlich, J., Gussone, N., Berndt, J., Arlinghaus, H. F., and Dieckmann, G. S.: Salinity effects on cultured *Neogloboquadrina pachyderma* (sinistral) from high latitudes: new paleoenvironmental insights, Geo-Marine Letters, 41, 10.1007/s00367-020-00677-1, 2021.

Branson, O., Chauhan, N., Evans, D., Foster, G. L., and Rickaby, R. E. M.: Geochemical tracers of biomineralisation processes, in: Treatise on Geochemistry (Third edition), edited by: Anbar, A., and Weis, D., Elsevier, Oxford, 177–235, https://doi.org/10.1016/B978-0-323-99762-1.00128-5, 2025.

Chaabane, S., Garidel-Thoron, T., Meilland, J., Sulpis, O., Chalk, T., Brummer, G.-J., Mortyn, P., Giraud, X., Helene, H., Casajus, N., Kuroyanagi, A., Beaugrand, G., and Schiebel, R.: Migrating is not enough for modern planktonic foraminifera in a changing ocean, Nature, 1–7, 10.1038/s41586-024-08191-5, 2024.

Davis, C. V., Fehrenbacher, J. S., Hill, T. M., Russell, A. D., and Spero, H. J.: Relationships Between Temperature, pH, and Crusting on Mg/Ca Ratios in Laboratory-Grown *Neogloboquadrina* Foraminifera, Paleoceanography, 32, 1137–1152, 10.1002/2017pa003111, 2017.

Davis, C. V., Livsey, C. M., Palmer, H., Hull, P., Thomas, E., Hill, T. M., and Benitez-Nelson, C.: Extensive morphological variability in asexually produced planktic foraminifera, Science Advances, 6, 2020.

de Nooijer, L. J., Toyofuku, T., and Kitazato, H.: Foraminifera promote calcification by elevating their intracellular pH, Proceedings of the National Academy of Sciences, 106, 15374–15378, 10.1073/pnas.0904306106, 2009.

de Nooijer, L. J., Spero, H. J., Erez, J., Bijma, J., and Reichart, G. J.: Biomineralization in perforate foraminifera, Earth-Science Reviews, 135, 48–58, https://doi.org/10.1016/j.earscirev.2014.03.013, 2014.

https://doi.org/10.5194/egusphere-2026-2415
Preprint. Discussion started: 6 May 2026
© Author(s) 2026. CC BY 4.0 License.

644 Dickson, A. G., Sabine, C. L., and Christian, J. R., Dickson, A. G., Sabine, C. L., and Christian, J. R. (Eds.):
645 Guide to best practices for ocean CO2 measurement, PICES Special Publication 3; IOCCP Report 8,
646 North Pacific Marine Science Organization, Sidney, British Columbia, 191 pp., 10.25607/obp-1342,
647 2007.

648 Elderfield, H. and Ganssen, G.: Past temperature and δ18O of surface ocean waters inferred from
649 foraminiferal Mg/Ca ratios, Nature, 405, 442–445, 10.1038/35013033, 2000.

650 Evans, D., Müller, W., and Erez, J.: Assessing foraminifera biomineralisation models through trace
651 element data of cultures under variable seawater chemistry, Geochimica et cosmochimica acta, 236,
652 198–217, 10.1016/j.gca.2018.02.048, 2018.

653 Evans, D., Wade, B. S., Henehan, M., Erez, J., and Müller, W.: Revisiting carbonate chemistry controls
654 on planktic foraminifera Mg / Ca: implications for sea surface temperature and hydrology shifts over
655 the Paleocene–Eocene Thermal Maximum and Eocene–Oligocene transition, Clim. Past, 12, 819–835,
656 10.5194/cp-12-819-2016, 2016.

657 Eynaud, F., Cronin, T. M., Smith, S. A., Zaragosi, S., Mavel, J., Mary, Y., Mas, V., and Pujol, C.:
658 Morphological variability of the planktonic f oraminif er Neogloboquadrina pachyderma from ACEX
659 cores: Implications for Late Pleistocene circulation in the Arctic Ocean, Micropaleontology, 55, 101–
660 116, 10.2307/40607109, 2009.

661 Ezat, M., Meilland, J., Westgård, A., Chalk, T., Sykes, F., El Bani Altuna, N., Nadar, P., Tell, F., and de la
662 Vega, E.: CAGE-ARCLIM cruise: Culturing (sub)Arctic planktic foraminifera Neogloboquadrina
663 pachyderma and Globigerina bulloides: Implications for ocean acidification and paleoceanography
664 reconstructions, CAGE – Centre for Arctic Gas Hydrate, Environment and Climate Report Series, 10,
665 10.7557/cage.6768, 2022.

666 Ezat, M. M., Fahl, K., and Rasmussen, T. L.: Arctic freshwater outflow suppressed Nordic Seas
667 overturning and oceanic heat transport during the Last Interglacial, Nature Communications, 15,
668 8998, 10.1038/s41467-024-53401-3, 2024.

669 Ezat, M. M., Rasmussen, T. L., Hönisch, B., Groeneveld, J., and Demenocal, P.: Episodic release of CO2
670 from the high-latitude North Atlantic Ocean during the last 135 kyr, Nature Communications, 8,
671 14498, 10.1038/ncomms14498, 2017.

672 Ezat, M. M., Meilland, J., Westgård, A., Chalk, T. B., Rasmussen, T. L., El Bani Altuna, N., and
673 Lockwood-Ireland, C.: Cruise Report: CAGE21-2- Planktic foraminifera sampling for culturing
674 experiments, central Greenland Sea 75°N, Department of Geosciences, UiT The Arctic University of
675 Norway, N-9037 Tromsø, 10.7557/cage.6714, 2021.

676 Fransson, A., Chierici, M., Miller, L. A., Carnat, G., Shadwick, E., Thomas, H., Pineault, S., and
677 Papakyriakou, T. N.: Impact of sea-ice processes on the carbonate system and ocean acidification at
678 the ice-water interface of the Amundsen Gulf, Arctic Ocean, Journal of Geophysical Research: Oceans,
679 118, 7001–7023, 10.1002/2013jc009164, 2013.

680 François, D., Reichart, G.-J., and de Nooijer, L. J.: Open or closed: pH modulation and calcification by
681 foraminifera, Science Advances, 11, eadq8425, doi:10.1126/sciadv.adq8425, 2025.

682 Fritz-Endres, T. and Fehrenbacher, J.: Preferential Loss of High Trace Element Bearing Inner Calcite in
683 Foraminifera During Physical and Chemical Cleaning, Geochemistry, geophysics, geosystems : G3, 22,
684 n/a, 10.1029/2020GC009419, 2021.

https://doi.org/10.5194/egusphere-2026-2415
Preprint. Discussion started: 6 May 2026
© Author(s) 2026. CC BY 4.0 License.

Greco, M., Jonkers, L., Kretschmer, K., Bijma, J., and Kucera, M.: Depth habitat of the planktonic foraminifera *Neogloboquadrina pachyderma* in the northern high latitudes explained by sea-ice and chlorophyll concentrations, Biogeosciences, 16, 3425–3437, 10.5194/bg-16-3425-2019, 2019.

Greco, M., Westgård, A., Sykes, F. E., Ezat, M. M., and Meilland, J.: Uncovering hidden structures: previously undescribed pseudopodia and ectoplasmic structures in planktonic foraminifera, Journal of Plankton Research, 10.1093/plankt/fbad031, 2023.

Guo, M. K. and Messer, H. H.: A comparison of Ca2+-, Mg2+-ATPase and alkaline phosphatase activities of rat incisor pulp, Calcified Tissue Research, 26, 33–38, 10.1007/BF02013231, 1978.

Haynes, L. L., Hönisch, B., Holland, K., Eggins, S., and Rosenthal, Y.: Calibrating Non-Thermal Effects on Planktic Foraminiferal Mg/Ca for Application Across the Cenozoic, Paleoceanography and Paleoclimatology, 38, https://doi.org/10.1029/2023PA004613, 2023.

Holland, K., Branson, O., Haynes, L. L., Hönisch, B., Allen, K. A., Russell, A. D., Fehrenbacher, J. S., Spero, H. J., and Eggins, S. M.: Constraining multiple controls on planktic foraminifera Mg/Ca, Geochimica et Cosmochimica Acta, 273, 116–136, 10.1016/j.gca.2020.01.015, 2020.

Hou, S., Toebrock, L., van der Linden, M., Rothstegge, F., Ziegler, M., Lourens, L. J., and Bijl, P. K.: Southern Ocean control on atmospheric CO2 changes across late Pliocene Marine Isotope Stage M2, Clim. Past, 21, 79–93, 10.5194/cp-21-79-2025, 2025.

Hupp, B. N. and Fehrenbacher, J. S.: Geochemical differences between alive, uncrusted and dead, crusted shells of Neogloboquadrina pachyderma: Implications for paleoreconstruction, Paleoceanography and Paleoclimatology, 34, e2023PA004638, https://doi.org/10.1029/2023PA004638, 2023.

Hupp, B. N. and Fehrenbacher, J. S.: Intratest trace element variability in polar and subpolar planktic foraminifera: insights into vital effects, ontogeny, and biomineralization processes, Journal of Foraminiferal Research, 54, 355–374, 10.61551/gsjfr.54.4.355, 2024.

Hönisch, B., Allen, K. A., Lea, D. W., Spero, H. J., Eggins, S. M., Arbuszewski, J., deMenocal, P., Rosenthal, Y., Russell, A. D., and Elderfield, H.: The influence of salinity on Mg/Ca in planktic foraminifers – Evidence from cultures, core-top sediments and complementary δ18O, Geochimica et Cosmochimica Acta, 121, 196–213, 10.1016/j.gca.2013.07.028, 2013.

Ingvaldsen, R. B., Assmann, K. M., Primicerio, R., Fossheim, M., Polyakov, I. V., and Dolgov, A. V.: Physical manifestations and ecological implications of Arctic Atlantification, Nature Reviews Earth & Environment, 10.1038/s43017-021-00228-x, 2021.

Inoue, M., Nohara, M., Okai, T., Suzuki, A., and Kawahata, H.: Concentrations of Trace Elements in Carbonate Reference Materials Coral JCp-1 and Giant Clam JCt-1 by Inductively Coupled Plasma-Mass Spectrometry, Geostandards and Geoanalytical Research, 28, 411–416, https://doi.org/10.1111/j.1751-908X.2004.tb00759.x, 2004.

Jacob, D. E., Wirth, R., Agbaje, O. B. A., Branson, O., and Eggins, S. M.: Planktic foraminifera form their shells via metastable carbonate phases, Nature Communications, 8, 10.1038/s41467-017-00955-0, 2017.

Jochum, K. P., Nohl, U., Herwig, K., Lammel, E., Stoll, B., and Hofmann, A. W.: GeoReM: A New Geochemical Database for Reference Materials and Isotopic Standards, Geostandards and Geoanalytical Research, 29, 333–338, https://doi.org/10.1111/j.1751-908X.2005.tb00904.x, 2005.

https://doi.org/10.5194/egusphere-2026-2415
Preprint. Discussion started: 6 May 2026
© Author(s) 2026. CC BY 4.0 License.

Jonkers, L., Buse, B., Brummer, G.-J. A., and Hall, I. R.: Chamber formation leads to Mg/Ca banding in the planktonic foraminifer Neogloboquadrina pachyderma, Earth and planetary science letters, 451, 177–184, 10.1016/j.epsl.2016.07.030, 2016.

Jonkers, L., Jiménez-Amat, P., Mortyn, P. G., and Brummer, G.-J. A.: Seasonal Mg/Ca variability of N. pachyderma (s) and G. bulloides: Implications for seawater temperature reconstruction, Earth and Planetary Science Letters, 376, 137–144, https://doi.org/10.1016/j.epsl.2013.06.019, 2013.

Kohfeld, K. E., Fairbanks, R. G., Smith, S. L., and Walsh, I. D.: *Neogloboquadrina pachyderma*(sinistral coiling) as paleoceanographic tracers in polar oceans: Evidence from northeast water polynya plankton tows, sediment traps, and surface sediments, Paleoceanography, 11, 679–699, 10.1029/96pa02617, 1996.

Kozdon, R., Eisenhauer, A., Weinelt, M., Meland, M. Y., and Nürnberg, D.: Reassessing Mg/Ca temperature calibrations of *Neogloboquadrina pachyderma* (sinistral) using paired $\delta^{44/40}$Ca and Mg/Ca measurements, Geochemistry, Geophysics, Geosystems, 10, n/a–n/a, 10.1029/2008gc002169, 2009a.

Kozdon, R., Ushikubo, T., Kita, N. T., Spicuzza, M., and Valley, J. W.: Intratest oxygen isotope variability in the planktonic foraminifer N. pachyderma: Real vs. apparent vital effects by ion microprobe, Chemical Geology, 258, 327–337, 10.1016/j.chemgeo.2008.10.032, 2009b.

Kucera, M.: Chapter Six Planktonic Foraminifera as Tracers of Past Oceanic Environments, in: Developments in Marine Geology, edited by: Hillaire–Marcel, C., and De Vernal, A., Elsevier, 213–262, https://doi.org/10.1016/S1572-5480(07)01011-1, 2007.

Kucera, M., Weinelt, M., Kiefer, T., Pflaumann, U., Hayes, A., Weinelt, M., Chen, M.-T., Mix, A. C., Barrows, T. T., Cortijo, E., Duprat, J., Juggins, S., and Waelbroeck, C.: Reconstruction of sea-surface temperatures from assemblages of planktonic foraminifera: multi-technique approach based on geographically constrained calibration data sets and its application to glacial Atlantic and Pacific Oceans, Quaternary Science Reviews, 24, 951–998, https://doi.org/10.1016/j.quascirev.2004.07.014, 2005.

Lea, D. W., Mashiotta, T. A., and Spero, H. J.: Controls on magnesium and strontium uptake in planktonic foraminifera determined by live culturing, Geochimica et Cosmochimica Acta, 63, 2369–2379, 0016-7037/99, 1999.

Lee, P.-T., Ho, S. L., Groeneveld, J., Mohtadi, M., Shen, C.-C., and Su, C.-C.: Effect of Cleaning Procedures on the Mg/Ca Ratio of Single-Specimen Planktic Foraminifera, Geochemistry, Geophysics, Geosystems, 26, e2024GC011975, https://doi.org/10.1029/2024GC011975, 2025.

Livsey, C. M., Kozdon, R., Bauch, D., Brummer, G. J. A., Jonkers, L., Orland, I., Hill, T. M., and Spero, H. J.: High-Resolution Mg/Ca and δ18O Patterns in Modern *Neogloboquadrina pachyderma* From the Fram Strait and Irminger Sea, Paleoceanography and Paleoclimatology, 35, https://doi.org/10.1029/2020PA003969, 2020.

Manno, C., Morata, N., and Bellerby, R.: Effect of ocean acidification and temperature increase on the planktonic foraminifer *Neogloboquadrina pachyderma* (sinistral), Polar Biology, 35, 1311–1319, 10.1007/s00300-012-1174-7, 2012.

Meilland, J., Ezat, M. M., Westgård, A., Manno, C., Morard, R., Siccha, M., and Kucera, M.: Rare but persistent asexual reproduction explains the success of planktonic foraminifera in polar oceans, Journal of Plankton Research, 10.1093/plankt/fbac069, 2022.

https://doi.org/10.5194/egusphere-2026-2415
Preprint. Discussion started: 6 May 2026
© Author(s) 2026. CC BY 4.0 License.

768 Morley, A., de la Vega, E., Raitzsch, M., Bijma, J., Ninnemann, U., Foster, G. L., Chalk, T. B., Meilland, J.,
769 Cave, R. R., Büscher, J. V., and Kucera, M.: A solution for constraining past marine Polar Amplification,
770 Nature Communications, 15, 9002, 10.1038/s41467-024-53424-w, 2024.

771 Okai, T., Suzuki, A., Kawahata, H., Terashima, S., and Imai, N.: Preparation of a New Geological Survey
772 of Japan Geochemical Reference Material: Coral JCp-1, Geostandards Newsletter, 26, 95–99,
773 https://doi.org/10.1111/j.1751-908X.2002.tb00627.x, 2002.

774 Olsen, A., Lange, N., Key, R. M., Tanhua, T., Bittig, H. C., Kozyr, A., Álvarez, M., Azetsu-Scott, K., Becker,
775 S., Brown, P. J., Carter, B. R., Cotrim da Cunha, L., Feely, R. A., van Heuven, S., Hoppema, M., Ishii, M.,
776 Jeansson, E., Jutterström, S., Landa, C. S., Lauvset, S. K., Michaelis, P., Murata, A., Pérez, F. F., Pfeil, B.,
777 Schirnick, C., Steinfeldt, R., Suzuki, T., Tilbrook, B., Velo, A., Wanninkhof, R., and Woosley, R. J.: An
778 updated version of the global interior ocean biogeochemical data product, GLODAPv2.2020, Earth
779 Syst. Sci. Data, 12, 3653–3678, 10.5194/essd-12-3653-2020, 2020.

780 Paton, C., Hellstrom, J., Paul, B., Woodhead, J., and Hergt, J.: Iolite: Freeware for the visualisation and
781 processing of mass spectrometric data, Journal of Analytical Atomic Spectrometry, 26, 2508–2518,
782 10.1039/C1JA10172B, 2011.

783 Paul, B., Petrus, J., Savard, D., Woodhead, J., Hergt, J., Greig, A., Paton, C., and Rayner, P.: Time
784 resolved trace element calibration strategies for LA-ICP-MS, Journal of Analytical Atomic
785 Spectrometry, 38, 1995–2006, 10.1039/D3JA00037K, 2023.

786 Peral, M., Bassinot, F., Daëron, M., Blamart, D., Bonnin, J., Jorissen, F., Kissel, C., Michel, E.,
787 Waelbroeck, C., Rebaubier, H., and Gray, W. R.: On the combination of the planktonic foraminiferal
788 Mg/Ca, clumped (Δ47) and conventional (δ18O) stable isotope paleothermometers in
789 palaeoceanographic studies, Geochimica et cosmochimica acta, 339, 22–34,
790 10.1016/j.gca.2022.10.030, 2022.

791 Pierrot, D., Lewis, E., and Wallace, D.: CO2SYS DOS Program developed for CO2 system calculations,
792 ORNL/CDIAC-105. Carbon Dioxide Information Analysis Center, Oak Ridge National Laboratory, US
793 Department of Energy, Oak Ridge, TN, 2006.

794 Prabhakar, M., Thirumalai, K., Cronin, T. M., Gemery, L., Thomas, E. K., and Rafter, P. A.: Morphotypical
795 and Geochemical Variations of Planktic Foraminiferal Species in Siberian and Central Arctic Ocean
796 Core Tops, Journal of Foraminiferal Research, 54, 1–19, 10.61551/gsjfr.54.1.1, 2024.

797 RCoreTeam: R: A Language and Environment for Statistical Computing, R Foundation for Statistical
798 Computing [code], 2022.

799 Rodríguez-Sanz, L., Graham Mortyn, P., Martínez-Garcia, A., Rosell-Melé, A., and Hall, I. R.: Glacial
800 Southern Ocean freshening at the onset of the Middle Pleistocene Climate Transition, Earth and
801 Planetary Science Letters, 345-348, 194–202, https://doi.org/10.1016/j.epsl.2012.06.016, 2012.

802 Russell, A. D., Hönisch, B., Spero, H. J., and Lea, D. W.: Effects of seawater carbonate ion concentration
803 and temperature on shell U, Mg, and Sr in cultured planktonic foraminifera, Geochimica et
804 Cosmochimica Acta, 68, 4347–4361, 10.1016/j.gca.2004.03.013, 2004.

805 Spindler, M. and Dieckmann, G. S.: Distribution and abundance of the planktic foraminifer
806 *Neogloboquadrina pachyderma* in sea ice of the Weddell Sea (Antarctica), Polar Biology, 5, 185–191,
807 10.1007/bf00441699, 1986.

https://doi.org/10.5194/egusphere-2026-2415
Preprint. Discussion started: 6 May 2026
© Author(s) 2026. CC BY 4.0 License.

Stein, R.: The Late Mesozoic-Cenozoic Arctic Ocean Climate and Sea Ice History: A Challenge for Past and Future Scientific Ocean Drilling, Paleoceanography and Paleoclimatology, 34, 1851–1894, https://doi.org/10.1029/2018PA003433, 2019.

Tell, F., Jonkers, L., Meilland, J., and Kucera, M.: Upper ocean flux of biogenic calcite produced by the Arctic planktonic foraminifera *Neogloboquadrina pachyderma*, 10.5194/bg-2022-59, 2022.

Tierney, J. E., Malevich, S. B., Gray, W., Vetter, L., and Thirumalai, K.: Bayesian Calibration of the Mg/Ca Paleothermometer in Planktic Foraminifera, Paleoceanography and Paleoclimatology, 34, 2005–2030, 10.1029/2019PA003744, 2019.

Toyofuku, T., Matsuo, M. Y., De Nooijer, L. J., Nagai, Y., Kawada, S., Fujita, K., Reichart, G.-J., Nomaki, H., Tsuchiya, M., Sakaguchi, H., and Kitazato, H.: Proton pumping accompanies calcification in foraminifera, Nature Communications, 8, 14145, 10.1038/ncomms14145, 2017.

Vázquez Riveiros, N., Govin, A., Waelbroeck, C., Mackensen, A., Michel, E., Moreira, S., Bouinot, T., Caillon, N., Orgun, A., and Brandon, M.: Mg/Ca thermometry in planktic foraminifera: Improving paleotemperature estimations for G. bulloides and N. pachyderma left, Geochemistry, Geophysics, Geosystems, 17, 1249–1264, https://doi.org/10.1002/2015GC006234, 2016.

Westgård, A., Ezat, M. M., Chalk, T. B., Chierici, M., Foster, G. L., and Meilland, J.: Large-scale culturing of Neogloboquadrina pachyderma, its growth in, and tolerance of, variable environmental conditions, Journal of Plankton Research, 10.1093/plankt/fbad034, 2023.

Westgård, A., Ezat, M. M., Sykes, F. E., Foster, G. L., Meilland, J., Chalk, T. B., and Milton, J. A.: Laboratory-grown crust in planktic foraminifera Neogloboquadrina pachyderma; insights into resolving inaccuracies in polar palaeotemperature estimates, Geochimica et Cosmochimica Acta, https://doi.org/10.1016/j.gca.2026.04.027, 2026.

Zeebe, R. E. and Sanyal, A.: Comparison of two potential strategies of planktonic foraminifera for house building: Mg2+ or H+ removal?, Geochimica et Cosmochimica Acta, 66, 1159–1169, https://doi.org/10.1016/S0016-7037(01)00852-3, 2002.